ADVANCED GIS

Advanced GIS

ADVANCED GIS

(VOLUME: 3, ISSUE: 2)

DECEMBER, 2023

Advanced GIS

ABOUT JOURNAL	**Advanced GIS (AGIS) journal** aims to publish original research articles, review articles and technical notes in the field of Geographic Information Systems (GIS). GIS allows spatial analysis, modeling and visualization of the environment. Nowadays, GIS is actively used in many fields such as agriculture, monitoring of natural disasters, ecology, climate change, polar studies, transportation, defense, education, environment, forest, together with remote sensing. In this context, the AGIS journal focuses on studies in the field of GIS. There is no page limit for the articles to be sent to the AGIS journal.

AIM & SCOPE

Advanced GIS

- To provide an easily accessible and wide-ranging discussion environment that will strengthen and accelerate the sharing of knowledge and experience between scientists, researchers, engineers, and other practitioners who are involved in direct or indirect activities with the following topics.

- To contribute to the initiation and development of inter-institutional cooperation, which is of great importance in terms of solving the problems related to professional developments that can play a role in technological and economic development in the world and Turkey

The scope of Advanced GIS Journal

- GIS, GPS, Remote Sensing and related geospatial studies

- Spatial data infrastructures; standardization and interoperability

- Spatiotemporal analysis

- Spatial Information Management

- 3D modeling and simulation

- Urban Planning Applications

- Disaster Management

- Climate Studies

- Cadastre Applications

- Desktop, mobile and Web-based spatial applications and services

Publication frequency	Biannual (June-December)
WEB	http://publish.mersin.edu.tr/index.php/agis/index
Contact	agis@mersin.edu.tr / mozgurcelik@mersin.edu.tr

Advanced GIS

EDITORIAL BOARD

Contents

Research Articles;

Review Article;

Determination of densities of existing intersection by buffer analysis (Samsun- Atakum intersections)

Aziz Uğur Tona*1 , **Erdem Emin Maraş**2 , **Vahdettin Demir**3

1Ondokuz Mayıs University, Faculty of Engineering, Department of Map Engineering, Samsun, Turkey
2Samsun University, Civil Aviation Academy, Department of Pilotage, Samsun, Turkey
3KTO Karatay University, Faculty of Engineering and Natural Sciences, Department of Civil Engineering, Konya, Turkey

ABSTRACT

This study was conducted to evaluate the traffic density of nine intersections located between the Highways intersection and the Toplu Konut Boulevard intersection on Atatürk Boulevard in Samsun's Atakum district, and to analyze the traffic flow in detail at these intersections. Analyzes were applied with ArcGIS 10.3 from GIS software. In the study, kernel density analysis was used to determine the densely populated areas, and buffer analysis was used to determine the density levels of intersections. Kernel density analysis was used to determine the density of settlements, then density maps were created depending on the buffer zones created by schools, institutions, hospitals and densely populated areas around the intersections. Buffer analysis was attempted at buffer sizes of 500 and 1000 meters and mapped in GIS software. As a result, it has been determined that the intersection with the least density is Vatan street intersection, and the ones with the highest density are YEDAŞ and Türk-iş intersection. Thus, a local problem was identified and solution suggestions were presented.

1. Introduction

Urban transportation is one of the most important requirements of modern life. However, urban traffic density can occasionally create significant problems. One of the biggest causes of these problems is traffic congestion at urban intersections. Insufficient road capacity, high number of vehicles, inadequate traffic management, and irregular parking are among the reasons for congestion at intersections. With population growth and rapid urban development, traffic density has become inevitable. This situation can occasionally lead to congestion and accidents at intersections. Nowadays, a significant portion of accidents and traffic congestion in urban road transportation occurs at urban intersections. Traffic congestion, which is the most important cause of urban transportation problems, can cause economic and social losses. These losses can affect not only time and money, but also human life. Therefore, handling intersections as a focal point of solutions is among the priority traffic elements (Oğuzhan, 2015). To evaluate traffic density, it is necessary to consider points with continuous traffic flow, such as residential areas, schools,

hospitals, and institutions. Determination of traffic density can be performed using geographic information systems (GIS) program.

GIS collects, processes and stores geographic data. GIS is an important tool in city planning. It is also a system that facilitates the arrangement, analysis and modeling of spatial data (Dogan & Yakar, 2018). It is used in various areas such as city management applications, traffic applications, infrastructure applications (Ernst et al, 2019). With GIS, density maps can be created and the busiest intersections can be detected. Traffic density maps help drivers learn about areas with high traffic density in earlier. As a result, it becomes possible to arrange intersections in a way that improves the flow of traffic.

Proximity analysis, also called buffer analysis, is the GIS querying for desired information within a certain geographic distance (Taşkaya & Ulutaş, 2021). Vector data is also performed with this analysis for point, line or polygon features. Buffer analysis is performed around a point with respect to a certain diameter, to the left or right of a line for a certain distance, or both, and inside or outside a polygon with respect to a certain distance. For example,

Cite this article

Tona, A. U., Maraş, E. E., & Demir, V. (2023). Determination of densities of existing intersection by buffer analysis (Samsun- Atakum intersections). *Advanced GIS*, 3(2), 39-46.

there are some uses that should not be used around a certain distance, such as base stations, schools, bridges, intersections, factories. It can be used for purposes such as detecting the buffer areas of these uses, identifying the misuses in these areas, guiding the decision-making mechanisms in the selection of a new application. It is possible to access the database information as well as the object information of the selected objects in the buffer zone (Belsis, 2023).

In recent years, GIS-based applications of buffer analysis in the scopus search base with a comprehensive perspective; it was searched with the keywords "buffer analysis" and "GIS" and 1519 published studies were identified with the article filter. These studies were examined in detail using the Voswiever program (Figure 1). In recent years, it has been determined by researchers that buffer analysis attracts attention in the fields of ecological network, rural settlements, accessibility, remote sensing land use and land cover and transportation.
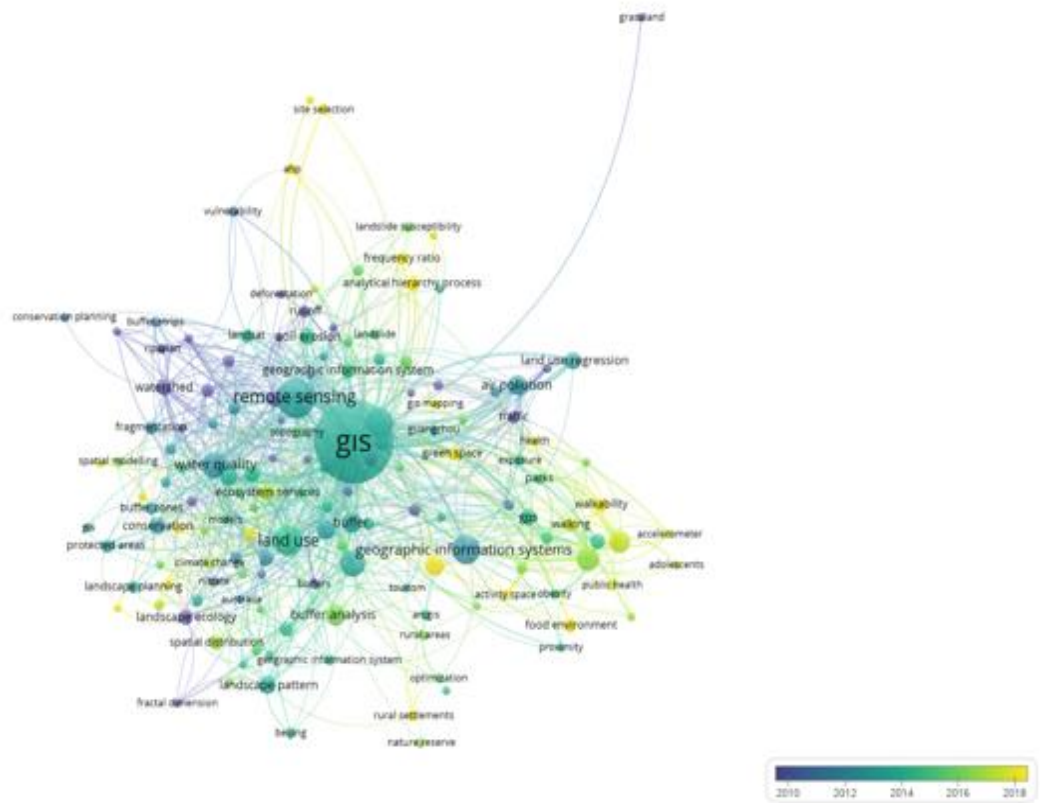
Figure 1. Keyword map of GIS based buffer analysis

In order to benefit from the traffic management and traffic signaling system of Samsun province, it is necessary to develop a new traffic-stimulated intersection model. The reason for this is that continuous stop-go is made at the intersections in the study area and the loss of time spent on the road reaches the highest points. As a result, people's patience in traffic decreases. In addition, fuel consumption increases due to the continuous stop-go operation of the vehicles at the lights, and excessive noise occurs due to reasons such as horn sound, engine noise, traffic accidents due to traffic density. In addition, the increase in fuel consumption causes more toxic gases to be emitted from vehicles and adversely affect the environment (Dönmez Akın, 2020). Zerenoğlu et al. (2022), by using the developed buffer analysis method, the relationship between traffic accidents in the intersection areas of shopping-education, transportation-education and transportation-shopping areas was examined. Using the optimized analysis method, hot spot analyzes of shopping-education, transportation shopping and transportation-education intersection areas were carried out. In the final analysis, traffic accidents occurring within 150 meters of

transportation, shopping, education, accommodation and food and beverage areas were examined. As a result of the study, it has been determined that traffic accidents occur mostly in the intersection areas of transportation and shopping areas among the daily activity areas. Sabel et al. (2005), the aim of their study is to determine traffic densities. GIS (Kernel Analysis) and Python programs were used in the study. As a result of the study, the accidents can not be predicted with GIS, but they stated that accident trends can be predicted. Karaman (2013), created a kernel density map according to the number of accident repetitions with a band width of 1000 and 1500 meters in Istanbul. As a result of the analysis, it has been determined that the regions with the highest number of accidents are around Şişli and Fatih districts on the European side. On the Anatolian side, the accidents were concentrated around Ataşehir.

The aim of this study is to analyze the intersections between highways intersection and Toplu Konut Boulevard intersection Junction located in Atakum district of Samsun province. In the density analysis, the images of the intersections in the study area were made with the help of drones. Kernel density analysis was used

to identify densely populated areas, and buffer analysis was used to determine the density levels of intersections.

2. Material and method

The data used in the study are in shape file format and were obtained from local governments. The base map used is the developing plan map and it is 1/1000 scaled.

The study focuses on nine intersections located on Atatürk Boulevard in Atakum district of Samsun. The study area is located between the highways intersection and the Toplu Konut Boulevard Intersection. Images taken with Google Earth and a drone for the study area are shown in Figure 2 and Figure 3-4, respectively
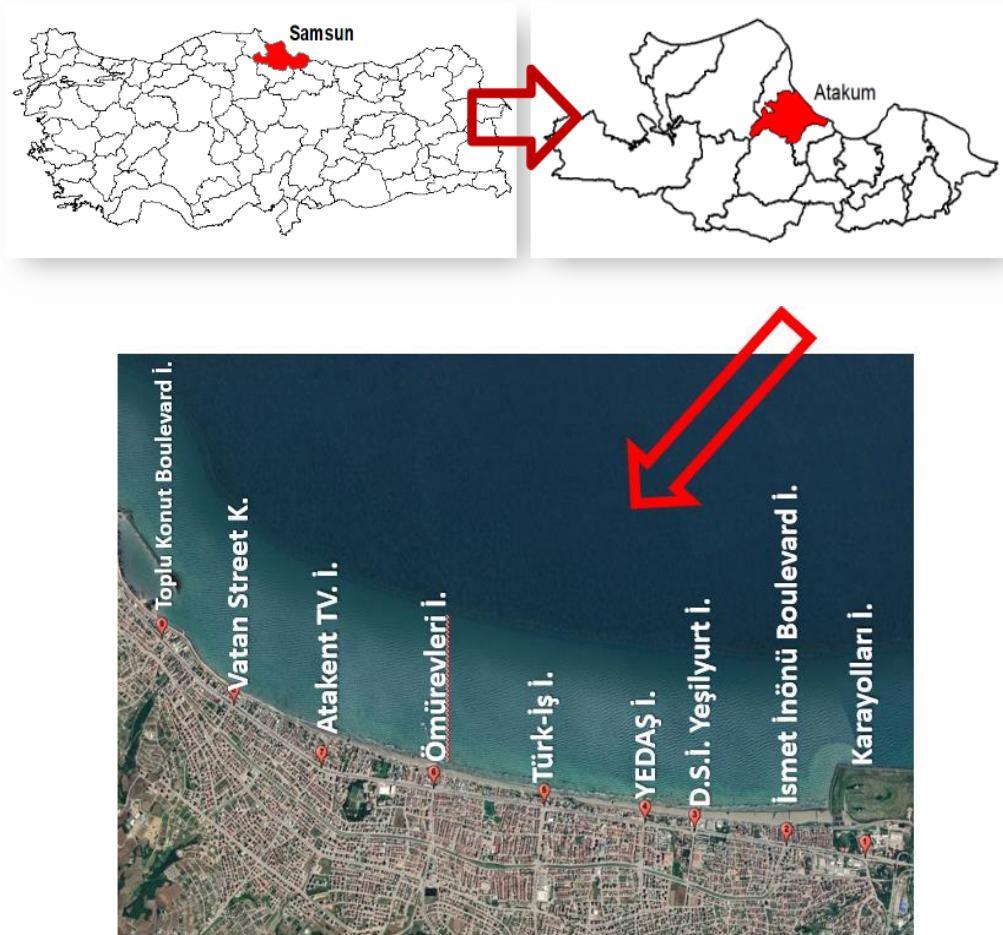
Figure 2. The study area (Google Earth, 2023)

In addition, drone images of 9 intersections in the study area are shown in Figure 4 – Figure 5. These drone images were taken from Samsun Metropolitan Municipality.

Figure 3. (a) View from the highways intersection to other intersections, (b) highways intersection
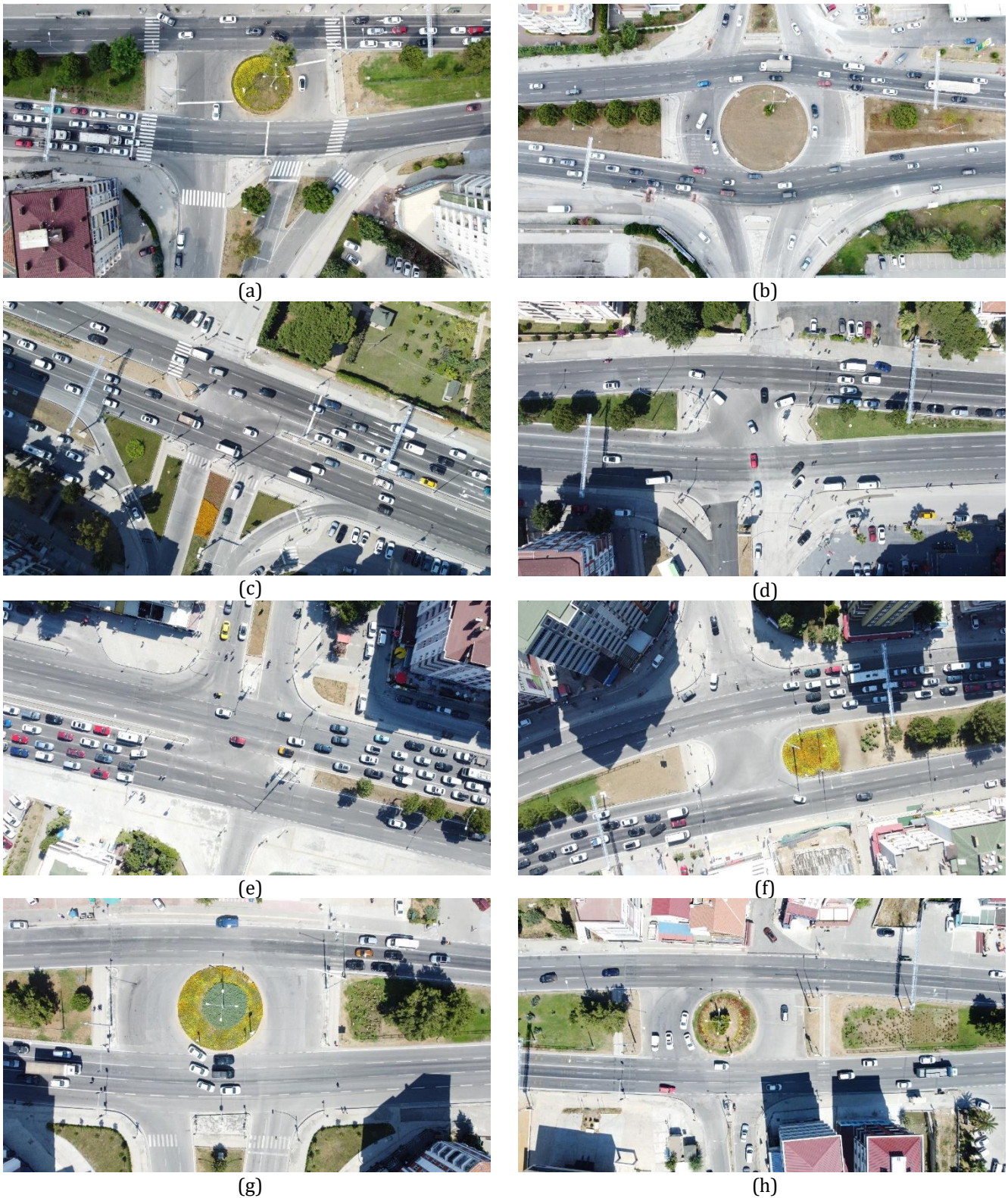
Figure 4. (a) İsmet İnönü boulevard intersection, (b) DSİ Yeşilyurt intersection, (c) YEDAŞ intersection, (d) Türk iş intersection, (e), Ömürevleri intersection, (f) Atakent tv intersection, (g) Vatan street intersection, (h) Toplu Konut boulevard intersection

In order to calculate the densities formed on these 9 intersections, the densely populated areas on the study area were determined by the kernel density analysis method, then the locations of the schools, hospitals and institutions on the study area were determined and transferred to the GIS software. These points have been preferred because they are the most frequently used locations in traffic. Since it is the place where people go most often, this will cause the density at the intersections to increase and the traffic to slow down. In order to determine the density levels of intersections, the parts of these points that intersect with the intersection should be determined. To achieve this, the buffer analysis method was used. Another reason for using buffer analysis is to reveal the most frequent and least preferred intersections in the study area. Schools, hospitals,

institutions and settlements in Atakum district layers are shown in Figure 5. The layers from the Google earth base were taken with their coordinates and integrated into the study. Kernel density analysis method and buffer analysis are explained in detail in the following sub-titles.
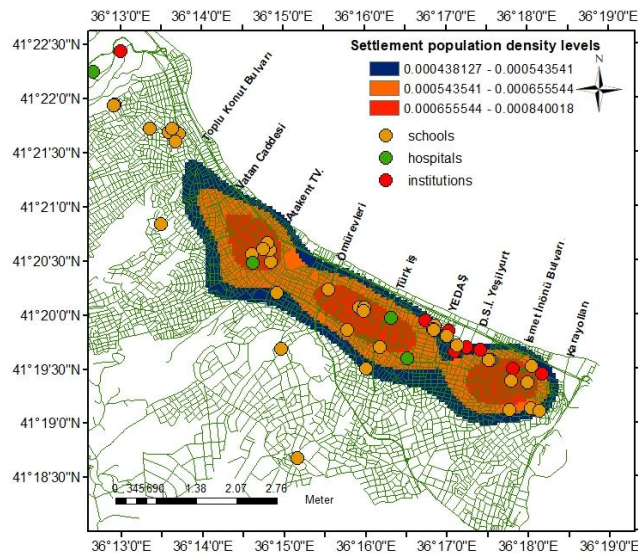
Figure 5. GIS view of schools, hospitals, settlements and institutions in Atakum district

2.1. Kernel density analysis

Kernel density analysis method is a method used to visualize the continuous distribution of data (Silverman, 1986). Linear data are related to the heights and shapes of the curves in the kernel density plot. In this method, the distribution frequency of the points is tested by comparing the observed frequency distribution with the expected value. On the other and point data, corresponds to the density of each point. It creates a grid by dividing the area of points with squares. Each square determines the density with a histogram according to the number of points falling within it (Toprak & Sunkar, 2022). Kernel density analysis refers to the density of points within the circle with a defined radius, instead of cells, and the point density that changes with distance from this source. This analysis method is used to measure the distribution of points in a more detailed and precise way (Bakak, 2016). In the kernel density analysis method, the surface value is highest at the point where the point is located and decreases as it moves away from the point. The search radius distance is the distance at which the kernel density reaches zero. This distance is a parameter used to calculate the density of the data. The kernel density tool calculates the density of the features on the map around these features. The formula used in the calculations of the densities is given in equation 1 (Toprak & Sunkar, 2022). As a result, a smooth, soft and curved surface is defined on each point (Tağil & Alevkayalı, 2013).

$$K(i) = \sum_{d<r} \frac{3}{\tau^2} (1 - \frac{d^2}{\tau^2})^2 \qquad (1)$$

Where K is kernel density value, d is the distance from event, and τ is bandwidth.

2.2. Buffer analysis

Buffer analysis is one of the most important parts of spatial analysis in GIS. Its main purpose can be defined as a regional area (creating buffer zones), out of a point, line or polygon, at a certain distance around the border. The commonly used name is buffer analysis (Yıldırım, 2016; Zhou et al., 2010; Huang et al., 2004; Dong et al., 2003). Considering the geographical features, a buffer zone is created around it at certain distances by using points and lines. Then, the details within the buffer zones are determined (Taşkaya & Ulutaş, 2021). With this analysis method, many things such as proximity to the road, distance, population density can be found. Buffer analysis can be performed in three different ways, as shown in Figure 6.
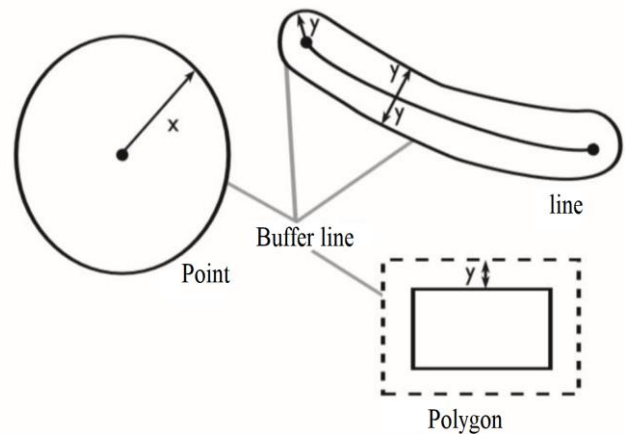
Figure 6. The various approaches in buffer analysis (Yıldırım, 2016)

Buffer analysis is applied in 3 different ways as point, line and polygon based. In this study, point-based buffer analysis method was used.

3. Application

Routes such as areas with frequently used schools, hospitals, institutions, and residential areas were marked on the land-use map, and the density on intersections within the study area was attempted to be identified using kernel density and buffer analysis method. The kernel density analysis method was used to show the density of settlement areas (Figure 7). By throwing points on the structures and giving coordinates, the areas where the pixel values of the analysis are intense were determined, then the regions where the settlements are dense were determined by the kernel density analysis method. To determine the buffer zones created by all of these layers on intersections, buffer analysis was applied with distances of 500 and 1000 meters, and the resulting density maps are shown in Figure 7 and Figure 8.
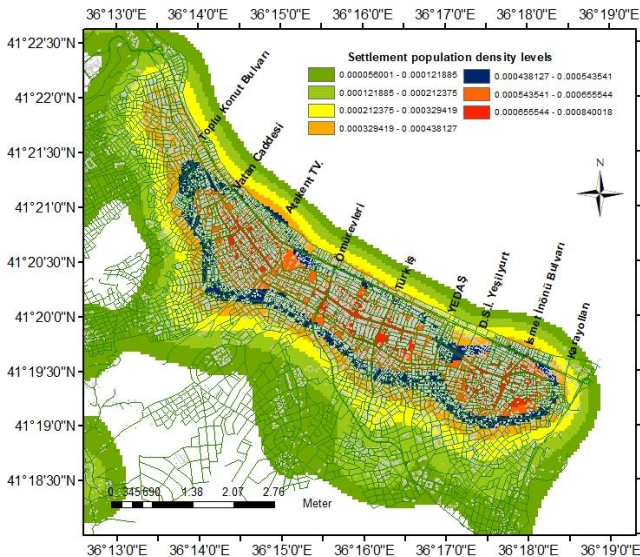
Figure 7. Settlement Kernel Density Analysis Map

In Figure 15, the most intense regions are shown in red, while the least dense regions are shown with green areas. The intensity values shown here are the representation of the pixel values formed according to the structure frequency obtained as a result of the analysis. The building densities increase from the blue colored area and the structuring gradually decreases outside the blue colored border. Therefore, the color blue was chosen as the border color at the density level of the settlement. The density levels of the settlements shown in Figure 8 are shown with the pixel values formed according to the frequency of the buildings. Kernel analysis was performed using spatial analysis tools-density-kernel density tabs in ArcGIS 10.3 software. Buffer analyzes of 500 and 1000 meters were applied to see significant intersections between the intersection dimensions and layers. Buffer analyzes of these dimensions are shown in Figure 9 and Figure 10.
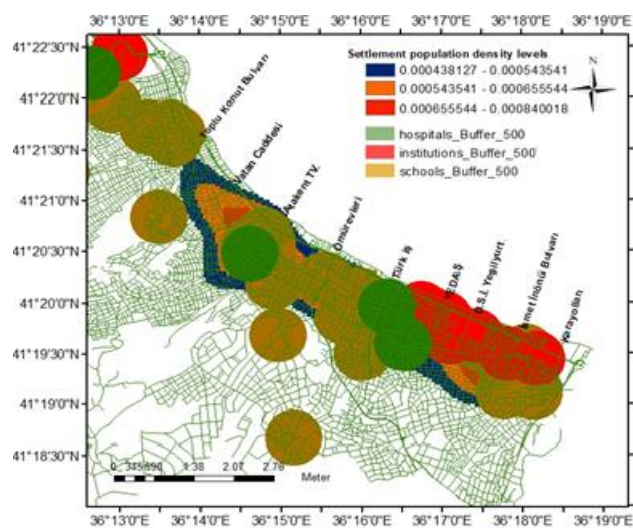
Figure 9. 500 Meter Buffer Analysis Map

In Figure 9, when the 500-meter buffer analysis is performed and the intersections are considered one by one, it is seen that the buffer zone of the institution layer coincides with the intersection at the Highways intersection. At İsmet İnönü boulevard, DSİ Yeşilyurt and

YEDAŞ intersections, school, residential and institution layers intersect. At Türk İş intersection, hospital and residential layers intersect. At Ömürevleri and Atakent Tv intersection, residential and school layers intersect. Finally, it was determined that the residential layer at Vatan street intersection and the buffer zones of the school layer at Toplu Konut Boulevard intersection coincide on the intersection.
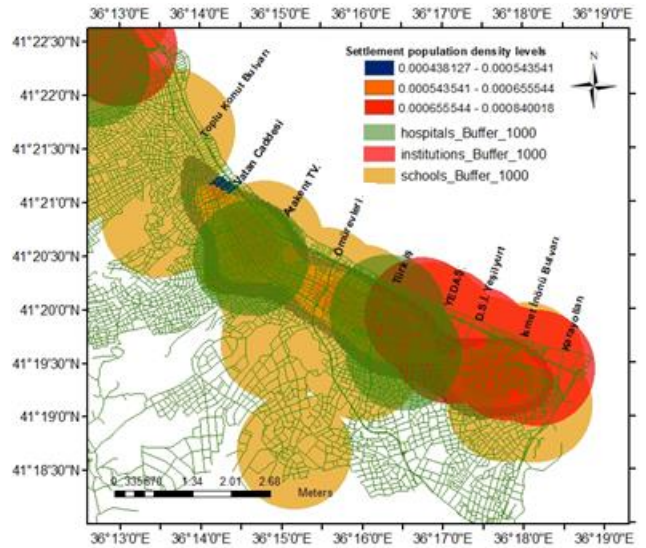
Figure 10. 1000 Meter Buffer Analysis Map

In Figure 10, when the 1000-meter buffer analysis is performed, the buffer zones belonging to the school, residential and institution layers at the highways intersection, the buffer zones belonging to the school, residential and institution layers at İsmet İnönü boulevard and DSİ Yeşilyurt intersections, buffer zones of school, residential and institution layers, buffer zones of hospital, school, residential and institution layers at YEDAŞ and Türk-iş intersections, buffer zones of school and residential layers at Ömürevleri intersection, buffer zones of school and residential layers at Atakent Tv intersection, It was observed that the buffer zones belonging to the residential and hospital layers, the buffer zones belonging to the school and residential layers at Vatan street intersection, and finally the buffer zones belonging to the school layer at the intersection of Toplu Konut Boulevard intersected and coincided on the intersection. Comparing the 500- and 1000-meter buffer analysis, the 500-meter buffer analysis was more in line with the kernel analysis indicators, while the 1000-meter buffer analysis showed intersections in a wider framework.

4. Discussion and conclusions

In this study, the density situations that occurred around the intersections of highways, İsmet İnönü boulevard, DSİ Yeşilyurt, YEDAŞ, Türk-iş, Ömürevleri, Atakent tv, Vatan street, and Toplu Konut boulevard, located on Atatürk boulevard in the Atakum district of Samsun, were examined using kernel density analysis and buffer analysis in a GIS environment. Settlement density was determined using kernel density analysis,

and then density maps were created based on the buffer zones around schools, institutions, hospitals, and areas with high population density. As a result of buffer analyses conducted at 500 and 1000 meters, it was observed that the Vatan Boulevard intersection had the least density, while the YEDAŞ and Türk iş intersections had the highest densities. Buffer analyzes of 500 and 1000 meters were made in order to show the intersections of the layers in a meaningful way at the intersections. These analyses enable the development of various models according to the density situations of intersections, and through these models, problems in crowded intersections can be identified and addressed. The densest regions in the obtained density maps are compatible with the literature (Dönmez Akın, 2020; Maraş, 2011). As a result, regulating traffic flow and reducing traffic congestion is an important factor in increasing the livability of cities. Towards this goal, considering many parameters such as the density situation of the intersection, the topography of the area, and the development status, different models can be implemented to make traffic more fluid. For example, an interchange can be built at the highways intersection, and a pedestrian overpass can be constructed at the Vatan Boulevard intersection. Depending on the overall perspective of the surrounding area, models such as interchanges, modern roundabouts, and pedestrian overpasses can be implemented around intersections. Conducting these studies will facilitate people's daily lives and help to make cities more livable. Also, the findings obtained as a result of the study can be generalized in different areas and used to investigate the traffic density problem.

Author Contributions

Aziz Uğur Tona: Literature review, field study, article writing. **Erdem Emin Maraş:** revision and interpretation. **Vahdettin Demir:** Editing, interpretation and revision.

Statement of Conflicts of Interest

There is no conflict of interest.

Statement of Research and Publication Ethics

Research and publication ethics were complied with in the study.

References

Bakak, Ö. (2016). The spatial evaluation of 2005 Sığacık Gulf (İzmir) Earthquakes. *Bulletin For Earth Sciences,* 37(1), 51-53. https://doi.org/10.17824/yrb.17485

Belsis. (2023). *GIS buffer analysis.* Retrieved May 5, 2023, from

http://www.belsiscad.com.tr/Urun/Tampon(Buffer)/14

Dogan, Y., & Yakar, M. (2018). GIS and three-dimensional modeling for cultural heritages. *International Journal of Engineering and Geosciences*, 3(2), 50-55. https://doi.org/10.26833/ijeg.378257

Dong, P., Yang, C., Rui, X., Zhang, L., & Cheng, Q. (2003). An effective buffer generation method in GIS. In IGARSS 2003. *Proceedings Book of IEEE International Geoscience and Remote Sensing Symposium*, Toulouse, France, 6, 3706-3708.

Dönmez Akın, M. 2020. *Micro Simulation Technique Modeling of Traffic on the Ataturk Highway of Samsun* (Publication No. 612000) [Master's Thesis, Ondokuz Mayıs University]. YÖK National Thesis Center.

Ernst, F., Erdoğan, S., & Bayram, Y. (2019). Human resource management using geographic information systems (GIS): an example from Turkish land registry directorates. *International Journal of Engineering and Geosciences*, 4 (2), 71-77. https://doi.org/10.26833/ijeg.450571

Google Earth. (2023). Google Earth. Retrieved May 5, 2023, from https://earth.google.com/web/

Huang, Y., Shekhar, S., & Xiong, H. (2004). Discovering colocation patterns from spatial data sets: a general approach. *Proceedings Book of IEEE Transactions on Knowledge and data engineering*, 16(12), 1472-1485.

Karaman, E. (2013). *Spatial analysis of the traffic accidents in İstanbul* (Publication No. 333786) [Master's Thesis, Fatih University]. YÖK National Thesis Center.

Maraş, E. E. (2011). *Production of noise maps in context with European Union requirements with the support of geographic information system: Samsun province example* (Publication No. 295904) [Doctoral Thesis, Yıldız Technical University]. YÖK National Thesis Center.

Oğuzhan, E. N. (2015). *Determining qualification of urban intersections with method of scoring design criterias: Ankara sample* (Publication No. 417047) [Master's Thesis, Gazi University]. YÖK National Thesis Center.

Sabel, E. C., Kingham, S., Nicholson, A., & Bartie, P. (2005, November 24-25). *Road Traffic Accident Simulation Modelling- A Kernel Estimation Approach.* [Symposium presentation]. The 17th Annual Colloquium of the Spatial Information Research Centre, University of Otago, New Zealand.

Silverman, B. W. (1986). *Density estimation for statistics and data analysis*. CRC press.

Tağil, Ş., Alevkayali, Ç. (2013). Earthquake spatial distribution in the egean region, Turkey: the geostatistical approach. *Journal of International Social Research*, 6(28), 369-379.

Taşkaya, S., & Ulutaş, N. (2021). Determining the Most Suitable Restaurant Areas for Investment by GIS, The case of Tunceli. *Osmaniye Korkut Ata University Journal of Natural and Applied Sciences,* 4(2), 134-141. https://doi.org/10.47495/okufbed.842696

Toprak, A., & Sunkar, M. (2022). Spatial and temporal analysis of natural disasters occurring in Ağrı

province. *Journal of Geography*, (44), 97-113. https://doi.org/10.26650/JGEOG2022-978387

Yıldırım, R.E. (2016). *Emergency response units event-location analysis with GIS: A case study of Samsun* (Publication No. 425836) [Master's Thesis Ondokuz Mayıs University]. YÖK National Thesis Center.

Zerenoğlu, H., Özlü, T., & Haybat, H. (2022). Relationship of Traffic Accidents Occurring in Antalya City with Daily Activity Areas. *Mavi Atlas,* 10(2), 509-531.

https://doi.org/10.18795/gumusmaviatlas.1131907

Zhou, G., Wang, L., Wang, D., & Reichle, S. (2010). Integration of GIS and data mining technology to enhance the pavement management decision making. *Journal of Transportation Engineering*, 136(4), 332-341. https://doi.org/10.1061/(ASCE)TE.1943-5436.0000092

Assessing hydrological modeling approaches: a review of the soil conservation service curve number and the soil and water assessment tool

Farhad Osman Omar[1, 2] , **Azad Rasul*[3]**

1Scientific Research Center, Soran University, Soran, Iraq
2Department of Tourism Foundation Administrations, Erbil Administrative Technical Institute, Erbil Polytechnic University, Erbil, Iraq
3Faculty of Arts, Department of Geography, Soran University, Soran, Iraq

check for updates

ABSTRACT

This article reviews two hydrological modeling tools, the Soil Conservation Service Curve Number (SCS-CN) model and the Soil and Water Assessment Tool (SWAT), and the Analytic Hierarchy Process (AHP) method used for estimating surface runoff and evaluating the impacts of land use changes on watershed responses. The SCS-CN model has been widely used for estimating surface runoff from rainfall, and its integration with GIS and remote sensing has improved its accuracy and precision. The SWAT model has also been effective in assessing the impact of land cover and land use changes on hydrologic response. The AHP method has been used to suggest the best locations for rainfall water harvesting in arid regions. However, these models also have limitations that should be considered when applying them to different watersheds. Proper calibration and validation of the models' input parameters are crucial to ensure accurate results, and the models' performance can be affected by uncertainties in the input data and model parameterization. Despite these limitations, these tools remain useful for evaluating surface runoff and its impact on water resource management, flood control, erosion prevention, and sustainable land and water management practices. In conclusion, the SCS-CN model, SWAT model, and AHP method are important approaches to evaluate surface runoff and its impacts, but their limitations and suitability for different watersheds should be carefully considered.

1. Introduction

Hydrological modeling plays a crucial role in understanding the complex relationships between rainfall and runoff processes, enabling accurate assessments of surface runoff. This understanding is vital for effective catchment design, planning, and management. By enabling the estimation of continuous surface runoff and enhancing comprehension of catchment behaviors, hydrological modeling provides valuable insights.

This article reviews three hydrological modeling tools used for estimating surface runoff and evaluating the impacts of land use changes on watershed responses. The first tool reviewed is the Soil Conservation Service Curve Number (SCS-CN) model, which has been widely used for estimating surface runoff from rainfall. The second tool reviewed is the Soil and Water Assessment Tool (SWAT), which is commonly used to simulate hydrological processes and assess the impact of land use changes on hydrologic response. Finally, the third tool reviewed is the Analytic Hierarchy Process (AHP), which

has been used to suggest the best locations for rainfall water harvesting in arid regions. While these tools have been found to be effective for hydrological modeling, they also have limitations that should be considered when applying them to different watersheds. Proper calibration and validation of the models' input parameters are crucial to ensure accurate results, and the models' performance can be affected by uncertainties in the input data and model parameterization. Despite these limitations, these tools remain useful for evaluating surface runoff and its impact on water resource management, flood control, erosion prevention, and sustainable land and water management practices. Applying these models in hydrology analysis helps to better comprehend important natural disasters such as floods (Demir & Keskin, 2022).

A comprehensive literature search was conducted using various databases, including Web of Science, Scopus, and Google Scholar. The search was conducted using the following keywords: hydrological modeling, soil conservation service curve number, soil and water analyses tool, and analytic hierarchy process. The search was limited to articles published in peer-reviewed

journals from 2000 to 2023. The search also included relevant articles identified through the reference lists of the retrieved articles.

2. Methodology

2.1. Criteria selection

The articles were selected based on their relevance to the topic of hydrological modeling and the use of the Soil Conservation Service Curve Number model, the Soil and Water Analyses Tool, and the Analytic Hierarchy Process. The articles were screened by title, abstract, and full text, and only articles that met the inclusion criteria (relevance to the topic, peer-reviewed, and published from 2000 to 2013) were included in the review.

2.2. Data extraction and analysis

The articles were analyzed and summarized based on their research objectives, study area, modeling approach, input data sources, model parameterization, calibration, validation, and model performance evaluation. The strengths and weaknesses of each model were also identified and discussed. The extracted data were synthesized and presented in a narrative format.

2.3. Synthesis of findings

The findings from the selected articles were synthesized to provide an overview of the strengths and weaknesses of the Soil Conservation Service Curve Number model (Equations 1-3), the Soil and Water Assessment Tool, and the Analytic Hierarchy Process (Figure 1). The synthesis also identified the gaps in the current knowledge and the future research directions in hydrological modeling. The limitations of the models were discussed, and recommendations were made for improving their accuracy and applicability.

$$Q = \frac{(P - Ia)^2}{(P - Ia) + S} \tag{1}$$

where Q = Runoff depth (mm), P = Rainfall (mm), the maximum retention after runoff starts (S), and the initial abstraction (Ia).

$$Ia = 0.2S \tag{2}$$

The proportion of 0.2 is seldom changed.

Equation (3) establishes a connection between the potential maximum retention after runoff starts, represented as S, and the characteristics of the watershed's land use/vegetative cover and soil.

$$S = \frac{25200}{CN} - 25 \tag{3}$$
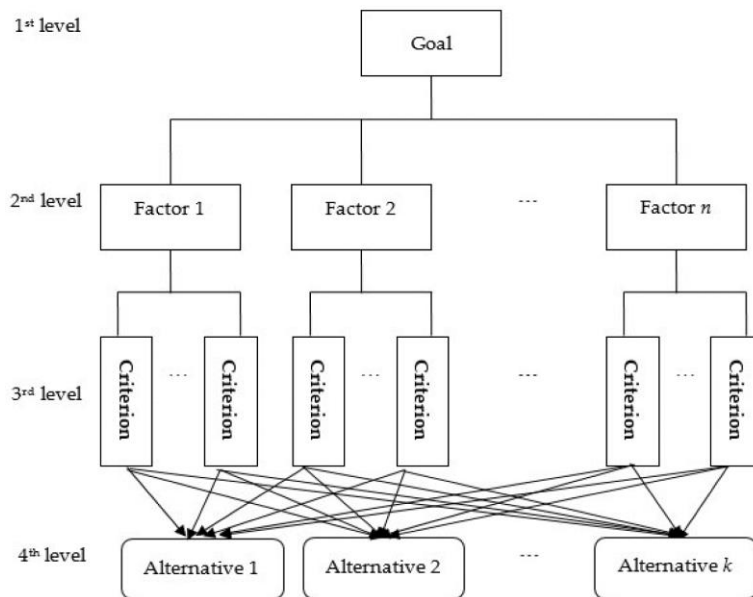
Figure 1. The structure of the analytic hierarchy process (Huang, 2021).

3. Surface water and soil conservation service curve number (SCS-CN)

The Soil Conservation Service Curve Number (SCS-CN) model is a popular and frequently used approach to evaluate surface runoff from rainfall. The model is based on land use and land cover (LULC), soil type, and soil moisture. Geographic Information System (GIS) can be used to merge maps with databases and estimate surface runoff. The integration of GIS and remote sensing can automate the surface runoff estimation depending on the SCS-CN model (Meshram et al., 2017; Weng, 2001). GIS

and remote sensing have been successfully utilized to manage non-spatial and spatial databases that illustrate the hydrological properties of watersheds.

Different models have been proposed to investigate the suitability of the SCS-CN model in various types of watersheds. In some watersheds, the response of linear runoff gives better outcomes than the SCS-CN model. The modified version of the SCS-CN model, known as the Mishra and Singh (MS model), integrates previous moisture in direct surface runoff calculations and manages distance better than the existing SCS-CN model (Karn et al., 2016; Suresh Babu & Mishra, 2012). The two-Curve Number approach is able to explain the CN-rainfall

variation observed in natural watersheds (Soulis & Valiantzas, 2012).

Remote sensing data with GIS and the SCS-CN method have been utilized to estimate runoff depth, weighted curve number, and volume of runoff in different watersheds. The SCS-CN model has been validated for urban areas, and with the help of RS data with GIS tools, the entire hydrological process can be simulated with higher precision, leading to more accurate results. However, substantial uncertainties exist in using the curve number model for estimating runoff from un-gauged watersheds (Tedela et al., 2012). Curve number selection requires independent calibration to watersheds representative of hydrologic characteristics and the regional landscape.

The Soil Conservation Service Curve Number (SCS-CN) model has been widely used for estimating surface runoff from rainfall. It has proven to be an effective method for hydrological modeling, and its integration with GIS and remote sensing has improved its accuracy and precision. The SCS-CN model has been successfully validated for urban areas, and its use has expanded to other types of watersheds. The model is also useful for the evaluation of land use and land cover changes and their impacts on surface runoff. The SCS-CN model's capability to provide precise estimates of surface runoff makes it a valuable tool for water resource management, flood control, and erosion prevention.

One of the limitations of the SCS-CN model is that it requires independent calibration to representative watersheds (Tedela et al., 2012). The SCS-CN model has been criticized for its lack of flexibility and simplicity, which hinders its suitability for various types of watersheds. The model's reliance on empirical relationships between curve numbers, rainfall, and runoff limits its ability to account for other hydrological processes, such as groundwater recharge and interflow. The SCS-CN model does not provide information on the quality of surface runoff, which can affect water supply and ecosystem services. As a result, the SCS-CN model's accuracy can be affected by uncertainties in the input parameters and assumptions.

In conclusion, the SCS-CN model is a useful tool for estimating surface runoff from rainfall, and its integration with GIS and remote sensing has improved its accuracy and precision. However, the model's limitations, such as its lack of flexibility and simplicity, reliance on empirical relationships, and uniform assumptions, should be considered when applying it to different watersheds (Table 1). Careful calibration and validation of the model's input parameters are required to ensure accurate results (Zlatanović & Gavrić, 2013). Despite its limitations, the SCS-CN model remains an important approach to evaluating surface runoff and is widely used in hydrological modeling and water resource management.

Table 1. Characteristics of reviewed Hydrological Models for Surface Runoff Estimation and Watershed Management in the study

Model	Purpose	Advantages	Limitations	Example Researches
Surface water and Soil Conservation Service Curve Number (SCS-CN)	The SCS-CN model is widely used for estimating surface runoff from rainfall. The model is based on land use and land cover (LULC), soil type, and soil moisture.	The SCS-CN model has been successfully validated for urban areas, and its use has expanded to other types of watersheds.	The model has limitations, such as its lack of flexibility and simplicity, reliance on empirical relationships, and uniform assumptions, which affect its accuracy.	"Runoff modeling using SCS-CN and GIS approach in the Tayiba Valley Basin, Abu Zenima area, South-west Sinai, Egypt "(Hagras, 2023); "Suitable site selection for rainwater harvesting and storage case study using Dohuk Governorate (Ibrahim et al., 2019) "
Soil and Water Assessment Tool (SWAT)	The SWAT model is widely utilized to estimate surface runoff and assess the impact of land use change on watershed responses.	The model has been effectively used in various hydrology studies, such as those examining the effects of land use changes on surface runoff.	The model's performance can be affected by uncertainties in the input data and model parameterization.	"Hydrological modeling with respect to impact of land-use and land-cover change on the runoff dynamics in Budhabalanga river basing using ArcGIS and SWAT model " (Bal et al., 2021); "Simulating streamflow in an ungauged catchment of Tonlesap Lake Basin in Cambodia using Soil and Water Assessment Tool (SWAT) model" (Ang & Oeurng, 2018)
Analytic Hierarchy Process (AHP)	The AHP is used to suggest the best locations for rainfall water harvesting in arid regions.	The model considers criteria such as rainfall intensity, soil type, land use, and topography to rank potential locations.	The AHP model has limitations, such as the need for careful calibration and validation, and the assumption of equal importance of criteria.	" The use of AHP within GIS in selecting potential sites for water harvesting sites in the Azraq Basin—Jordan" (Al-shabeeb, 2016); "Development and assessment of rainwater harvesting suitability map using analytical hierarchy process, GIS and RS techniques " (Balkhair & Ur Rahman, 2021)

4. Soil and water assessment tool (SWAT)

The Soil and Water Assessment Tool (SWAT) has been widely utilized in various hydrology studies to estimate surface runoff and the impacts of land use change on watershed responses. One such study by Yusuf et al. (2021) examined the effects of land use changes on surface runoff in the Bekasi River sub-watershed. The study utilized the SWAT model and the SCS Curve Number to analyze surface runoff and land use changes,

respectively. Similarly, Baker & Miller (2013) used the SWAT model to assess the impact of land cover and land use changes on the hydrologic response of the river Njoro watershed in Kenya's Rift Valley. In both studies, the SWAT model proved to be an effective tool for assessing the relative impact of land cover change on hydrologic response.

Another study by Basu et al. (2022) employed the SWAT model to evaluate the impact of landcover changes on runoff in Dublin, Ireland, spanning the period from 1993 to 2019. Their research highlights the importance of incorporating dynamic and time-varying landcover data into hydrological modeling to accurately simulate runoff. Iskender & Sajikumar (2016) compared the performance of the SWAT model and the Geomorphological Instantaneous Unit Hydrograph (GIUH) model in predicting surface runoff from ungagged basins. The study concluded that the GIUH model was marginally better than the SWAT model. Overall, the SWAT model has proven to be a valuable tool for hydrological modeling and can be used to assess the impact of land use changes on hydrological response in various watersheds.

The studies discussed highlight the versatility of the model and its applicability in different geographical regions. The use of the SWAT model in these studies has led to a better understanding of the impacts of land use change on hydrologic response, which is important for sustainable land and water management practices. The ability to assess the impact of land use changes on surface runoff and other hydrological processes using the SWAT model provides valuable information for policymakers, land managers, and water resource professionals.

One of the limitations of the SWAT model is the need for detailed input data, which can be time-consuming and expensive to obtain. This may limit the applicability of the model in regions where data is scarce or not readily available. Additionally, the model's performance can be affected by uncertainties in the input data and model parameterization. Proper calibration and validation of the model are crucial to ensure accurate simulations. Another limitation is that the model may not be able to capture the complex hydrological processes that occur in certain types of watersheds or landscapes, which can lead to inaccuracies in the model output. Despite these limitations, the SWAT model remains a useful tool for hydrological modeling and has the potential to contribute significantly to sustainable land and water management practices.

5. Water harvesting by using analytic hierarchy process (AHP)

Water harvesting is a critical undertaking in arid regions, and Analytic Hierarchy Process (AHP) has been used to suggest the best locations for rainfall water harvesting (RWH). The AHP method integrates researchers' criteria using GIS (Meşin & Demir, 2023), and it has been used to evaluate and optimize the management of gained rainwater collection systems in semi-arid areas. Adham et al. (2016) designed a methodology that can support designers and decision-makers to improve the performance of existing and new

rainwater harvesting sites. Al-Abadi et al. (2017) developed a GIS-based model that incorporates AHP and fuzzy logic to identify appropriate sites for water harvesting buildings. The model utilized five influential factors to develop the model, which includes surface runoff depth, distance, slope, hydrological soil group, and land cover to river intermittent. Wu et al. (2018) used the AHP technique to determine suitable locations, incorporating spatial information into six sub-criteria and two major decision criteria: socioeconomic and environmental. Physical features were land use, potential runoff, and distance from roads, soil texture, slope, and distance from agricultural land.

The suitability of the site for harvesting rainwater was also considered in the study by Ibrahim et al. (2019). The model combined several parameters, such as slope, runoff potential, soil quality, land cover/use, stream order, and hydrology, to determine the suitability of the site for harvesting rainwater. In the study by Rajasekhar et al. (2020), AHP was performed to identify the rainwater harvesting places and potential recharge zones using thematic layers such as vadose zone, drainage density, land use/land cover, soil, runoff, geology, and slope. Finally, Sayl et al. (2020) used a GIS-based approach with RS to identify the optimal sites for rainwater harvesting, and the results showed that the rank order method and variance inverse methods affected the ranking priority and considered all of the criteria that were sensitive to impact in the ranking process at the different levels compared to the methods of AHP and fuzzy AHP.

In summary, AHP method integrated with GIS has proven to be an effective and flexible approach in suggesting the best locations for water harvesting. The studies by Adham et al. (2016), Al-Abadi et al. (2017), Wu et al. (2018), Ibrahim et al. (2019), Rajasekhar et al. (2020), and Sayl et al. (2020) are examples of how AHP can be used to determine suitable locations for water harvesting by considering various factors such as socioeconomic and environmental aspects, surface runoff depth, distance, slope, hydrological soil group, land cover, runoff potential, soil quality, stream order, and hydrology. The utilization of AHP in combination with GIS provides a low-cost, time-saving, and flexible approach for decision-makers and designers to improve the performance of both existing and new water harvesting systems.

The utilization of AHP in water harvesting has demonstrated its usefulness in identifying suitable locations for water harvesting. By incorporating various criteria and factors, such as environmental, socioeconomic, and physical features, AHP provides a comprehensive approach to assess the feasibility and effectiveness of water harvesting systems. It helps decision-makers and designers to make informed decisions and optimize the performance of existing or new systems, leading to more efficient and sustainable water management in arid regions. Furthermore, AHP enables the integration of multiple stakeholder perspectives into the decision-making process, promoting consensus-building and stakeholder participation.

Despite the benefits of AHP, some limitations need to be considered. One limitation is that AHP requires considerable expertise in defining criteria, sub-criteria, and pairwise comparisons, which can be time-consuming and challenging. Moreover, AHP heavily relies on subjective judgments and preferences of decision-makers or stakeholders, which can introduce bias and uncertainty in the decision-making process. The availability and quality of data are also crucial in the AHP method, and inaccurate or incomplete data can lead to inaccurate results. Finally, AHP's complexity and technicality may pose challenges to its adoption by policymakers, practitioners, and stakeholders who lack technical expertise in GIS and AHP methods. Therefore, careful consideration and communication of the results and implications of AHP analyses are necessary to ensure its effectiveness and usability.

6. Future research directions

While the model is widely used in hydrological studies it has some gaps for instance the impact of rain intensities was not taken into consideration (Wang & Bi, 2020). Future research in hydrological modeling should focus on improving the accuracy and reliability of the Curve Number Model. This model has been effective in estimating surface runoff from rainfall, but uncertainties remain. Advancements could include incorporating other hydrological processes such as groundwater recharge and interflow, and improving the model's ability to account for variations in soil properties and land use.

Integrating multiple models could also enhance the accuracy and reliability of hydrological simulations. Future research should explore the potential of combining the SCS-CN model with other models, such as the SWAT model, the Geomorphological Instantaneous Unit Hydrograph (GIUH) model, and other models that can capture different hydrological processes.

Another important area for future research is improving data availability. The availability and quality of data, including meteorological data, soil data, and land use data, are often limited, especially in certain regions. Efforts should focus on improving the availability and quality of data to support more accurate hydrological modeling. Furthermore, incorporating uncertainty analysis in hydrological modeling can help assess the reliability and accuracy of models, accounting for uncertainties in input data, model parameterization, and assumptions. Lastly, the development of decision support systems that incorporate hydrological models could provide valuable information for water resource management and decision-making.

7. Conclusions

In conclusion, the Soil Conservation Service Curve Number (SCS-CN), the Soil and Water Assessment Tool (SWAT), and the Analytical Hierarchy Process (AHP) are three commonly used approaches in hydrological modeling. The SCS-CN model, when integrated with GIS and remote sensing, has proven to be an effective method for estimating surface runoff from rainfall and is widely used in water resource management, flood control, and erosion prevention. However, the model's limitations should be considered when applying it to different types of watersheds. The SWAT model has also been widely used in hydrological studies and has proven to be a valuable tool for assessing the impact of land use changes on hydrological response in various watersheds. Lastly, the AHP approach has been used to prioritize various factors affecting hydrological processes, such as land use and land cover changes, and can assist in decision-making processes related to water resource management. Overall, each approach has its strengths and limitations, and careful calibration and validation of input parameters are necessary for accurate results.

Author Contributions

Farhad Omar: Conceptualization, methodology, writing-reviewing and editing. **Azad Rasul:** Supervision, investigation, writing- original draft preparation.

Statement of Conflicts of Interest

There is no conflict of interest.

Statement of Research and Publication Ethics

Research and publication ethics were complied with in the study.

References

Adham, A., Riksen, M., Ouessar, M., & Ritsema, C. J. (2016). A methodology to assess and evaluate rainwater harvesting techniques in (semi-) arid regions. *Water*, 8(5), 198. https://doi.org/10.3390/w8050198

Al-Abadi, A. M., Shahid, S., Ghalib, H. B., & Handhal, A. M. (2017). A GIS-based integrated fuzzy logic and analytic hierarchy process model for assessing water-harvesting zones in Northeastern Maysan Governorate, Iraq. *Arabian Journal for Science and Engineering,* 42(6), 2487–2499. https://doi.org/10.1007/s13369-017-2487-1

Al-shabeeb, A. R. (2016). The use of AHP within GIS in selecting potential sites for water harvesting sites in the Azraq Basin—Jordan. *Journal of Geographic Information System*, 8(1), 73–88. https://doi.org/10.4236/jgis.2016.81008

Ang, R., & Oeurng, C. (2018). Simulating streamflow in an ungauged catchment of Tonlesap Lake Basin in Cambodia using soil and water assessment tool (SWAT) model. *Water Science*, 32(1), 89–101. https://doi.org/10.1016/j.wsj.2017.12.002

Baker, T. J., & Miller, S. N. (2013). Using the soil and water assessment tool (SWAT) to assess land use impact on water resources in an East African watershed. *Journal of Hydrology*, 486, 100–111. https://doi.org/10.1016/j.jhydrol.2013.01.041

Bal, M., Dandpat, A. K., & Naik, B. (2021). Hydrological modeling with respect to impact of land-use and land-cover change on the runoff dynamics in Budhabalanga River basing using ArcGIS and SWAT model. *Remote Sensing Applications: Society and Environment*, 23, 100527. https://doi.org/10.1016/j.rsase.2021.100527

Balkhair, K. S., & Ur Rahman, K. (2021). Development and assessment of rainwater harvesting suitability map using analytical hierarchy process, GIS and RS techniques. *Geocarto International,* 36(4), 421–448. https://doi.org/10.1080/10106049.2019.1608591

Basu, A. S., Gill, L. W., Pilla, F., & Basu, B. (2022). Assessment of variations in runoff due to landcover changes using the SWAT Model in an Urban River in Dublin, Ireland. *Sustainability*, 14(1), 534. https://doi.org/10.3390/su14010534

Demir, V., & Keskin, A. Ü. (2022). Flood flow calculation and flood modeling in rivers that do not have enough flow measurement (Samsun, Mert River sample). *Journal of Geomatics,* 7(2), 149–162. https://doi.org/10.29128/geomatik.918502

Hagras, A. (2023). Runoff modeling using SCS-CN and GIS approach in the Tayiba Valley Basin, Abu Zenima area, South-west Sinai, Egypt. *Modeling Earth Systems and Environment*, 1–13. https://doi.org/10.1007/s40808-023-01714-5

Huang, J.-J. (2021). Analytic hierarchy process with the correlation effect via WordNet. *Mathematics*, 9(8), 872. https://doi.org/10.3390/math9080872

Ibrahim, G. R. F., Rasul, A., Ali Hamid, A., Ali, Z. F., & Dewana, A. A. (2019). Suitable site selection for rainwater harvesting and storage case study using Dohuk Governorate. *Water*, 11(4), 864. https://doi.org/10.3390/w11040864

Iskender, I., & Sajikumar, N. (2016). Evaluation of surface runoff estimation in ungauged watersheds using SWAT and GIUH. *Procedia Technology*, 24, 109–115. https://doi.org/10.1016/j.protcy.2016.05.016

Karn, A. L., Lal, M., Mishra, S. K., Chaube, U. C., & Pandey, A. (2016). Evaluation of SCS-CN Inspired models and their comparison. *Journal of Indian Water Resources Society*, 36(3), 19–27.

Meshram, S. G., Sharma, S. K., & Tignath, S. (2017). Application of remote sensing and geographical information system for generation of runoff curve number*. Applied Water Science*, 7, 1773–1779. https://doi.org/10.1007/s13201-015-0350-7

Meşin, V., & Demir, V. (2023). Site selection for the technology development zone in Konya city center using geographic information systems-based analytical hierarchy method. Journal of Geomatics, 8(3), 208–221. https://doi.org/10.29128/geomatik.1161059

Rajasekhar, M., Gadhiraju, S. R., Kadam, A., & Bhagat, V. (2020). Identification of groundwater recharge-based potential rainwater harvesting sites for sustainable development of a semiarid region of southern India using geospatial, AHP, and SCS-CN approach. *Arabian Journal of Geosciences*, 13, 1–19. https://doi.org/10.1007/s12517-019-4996-6

Sayl, K., Adham, A., & Ritsema, C. J. (2020). A GIS-based multicriteria analysis in modeling optimum sites for rainwater harvesting. *Hydrology*, 7(3), 51. https://doi.org/10.3390/hydrology7030051

Soulis, K. X., & Valiantzas, J. D. (2012). SCS-CN parameter determination using rainfall-runoff data in heterogeneous watersheds–the two-CN system approach. *Hydrology and Earth System Sciences*, 16(3), 1001–1015. https://doi.org/10.5194/hess-16-1001-2012

Suresh Babu, P., & Mishra, S. K. (2012). Improved SCS-CN–inspired model. *Journal of Hydrologic Engineering,* 17(11), 1164–1172. https://doi.org/10.1061/(ASCE)HE.1943-5584.0000435

Tedela, N. H., McCutcheon, S. C., Campbell, J. L., Swank, W. T., Adams, M. B., & Rasmussen, T. C. (2012). Curve numbers for nine mountainous eastern United States watersheds: Seasonal variation and forest cutting. *Journal of Hydrologic Engineering*, 17(11), 1199–1203. https://doi.org/10.1061/(ASCE)HE.1943-5584.0000437

Wang, X., & Bi, H. (2020). The effects of rainfall intensities and duration on SCS-CN model parameters under simulated rainfall. *Water*, 12(6), 1595. https://doi.org/10.3390/w12061595

Weng, Q. (2001). Modeling urban growth effects on surface runoff with the integration of remote sensing and GIS. *Environmental Management*, 28, 737–748. https://doi.org/10.1007/s002670010258

Wu, R.-S., Molina, G. L. L., & Hussain, F. (2018). Optimal sites identification for rainwater harvesting in northeastern Guatemala by analytical hierarchy process. *Water Resources Management*, 32, 4139–4153. https://doi.org/10.1007/s11269-018-2050-1

Yusuf, S. M., Nugroho, S. P., Effendi, H., Prayoga, G., Permadi, T., & Santoso, E. N. (2021). Surface runoff of Bekasi River subwatershed. *IOP Conference Series: Earth and Environmental Science*, Indonesia, 744(1), 012108. https://doi.org/10.1088/1755-1315/744/1/012108

Zlatanović, N., & Gavrić, S. (2013). Comparison of an automated and manual method for calculating storm runoff response in ungauged catchments in Serbia. *Journal of Hydrology and Hydromechanics*, 61(3), 195–201. https://doi.org/10.2478/johh-2013-0025

A post earthquake damage assessment using GIS in district Mirpur, Pakistan

Warda Habib[1] , **Shakeel Mahmood*[1]** , **Noor ul Huda[1]** , **Siddra Noor[1]** , **Arslan Saleem[1]** , **Muhammad Siraj[1]** **Haseeb Ahmad[1]**

[1]Government College University, Department of Geography, Lahore, Pakistan

ABSTRACT

A moderate earthquake of magnitude Mw 5.6 struck the Kashmir region of Pakistan on September 24th, 2019, causing severe damage to buildings and infrastructure. The study aims to assess the extent of damage in Mirpur district, Azad Kashmir. In this research, the map of the affected area and damages is developed using Geographic Information System (GIS). Results indicated that damage to roads and houses is severe in the proximity of Mangla Dam. It was found from the analysis that shallow earthquakes with high magnitude can have disastrous consequences. It also poses the risk of Dam Lake Outburst Flooding (DLOF) which can cause disaster in the downstream regions. So, there is the utmost need to work on the mapping and hotspot analysis of the places susceptible to earthquakes. The result and findings of such a study can assist disaster management authorities and donor agencies reduce the risk of potential damage and suffering by preparing earthquake risk reduction plans and investments in disaster preparedness and prevention.

1. Introduction

Disasters are increasing tremendously over the earth resulting in high risks and vulnerabilities (Çelik & Yakar, 2023). Hydro-meteorological and geological hazards are common in South Asia (Rafi et al., 2022). Earthquakes are one of the most destructive and unpredictable geological hazards. Pakistan is also prone to earthquakes, floods, and landslides with different levels of vulnerabilities in both the rural and urban areas disrupting the physical, social, and economic environment (Ainuddin et al., 2014). Pakistan is a seismically active area that has experienced numerous earthquakes throughout history. (Stevenson et al., 2017).

Earthquakes leave a serious impact on the community (Wu et al., 2022). The cities located in the earthquake zone are exposed to earthquakes (Khan, 2021). The resilience of the community, infrastructure, and economy is playing a crucial role because it is indirectly related to vulnerability. The vulnerability of the community transforms hazard into disaster (Hidayat et al., 2020). Densely populated areas with a high density of infrastructure which are poorly prepared for such crises are more vulnerable and result in significant

mortality rates during unexpected catastrophes (Idris et al., 2022). These outcomes include physical destruction, adverse effects on the economy, and casualties (Sidi, 2017). Even though a tremor usually can last for a short time, the aftershocks could last for days, and the destruction is for a longer period (Kencanawati et al., 2020). Housing area security and seismic hazard analysis research are critical in designing sustainable reconstruction and decision-making, enhancing resilience, and limiting damages in densely populated regions (Mangkoesoebroto et al., 2019).

Pakistan is exposed to a variety of geo-environmental hazards (Sengara et al., 2016). Earthquakes are one of the geological hazards, leading to human life loss, and damage to property and infrastructure (Ahmed et al., 2022). Geologically, Pakistan lies in the region where the Indian, Eurasian, and Arabian tectonic plates interact and lead to earthquakes (Mikhail et al., 2019). Seismically, it is the active region having active faults (Gardezi et al., 2021). In the last eight decades, the country has been struck by many disastrous quakes including; the 1935-Quetta earthquake with a magnitude of 7.6 destroyed the historic city of Quetta, the 1947 Hunza Earthquake in

which 5300 people lost their lives and 17000 were injured, the 2005 Kashmir Earthquake in which more than 80 thousand people died and 3.5million loss their shelter (Lallemant et al., 2017). In the year 2013, district Awaran in Balochistan was struck by a sequence of two earthquakes that rocked the Awaran district within a span of 4 days (Shakya et al., 2021).

On September 24, 2019, a moderate yet severe earthquake of Mw 5.6 at a hypocentral depth of 10 km struck in the Kashmir Himalayas at the axis of Hazara Kashmir Syntaxis, because of reverse faulting convergent between the Indian and Eurasian plates (Gardezi et al., 2021). The tremors were felt in a radius of ~100km with damage taking place in the area of 700 km2 including human life losses. The epicenter was close to Mirpur in Kashmir, with a peak ground acceleration (PGA) of around 0.35 g (Khan et al., 2021).

The Mirpur Earthquake is the result of an onward collision between Indian and Eurasian plates on a main thrust fault namely the Samwal Fault in the epicentral region. Moreover, this earthquake caused several deaths and huge damage to the infrastructure in the epicentral zone (Sreejith et al., 2021). This study aims to assess the post-earthquake damages in Mirpur City, Azad Jammu Kashmir, Pakistan. The results of the study can be helpful for decision-making and further research on seismic risk assessment and reduction.

2. Study area

Mirpur is one of the districts in Azad Kashmir. Administratively, Mirpur is comprised of two sub-divisions namely Mirpur and Dadyal (Figure 1). Relatively, the study area is bounded by Kotli district in the north and east, by Potohar region (Punjab) in the west and Bhimber district in the south. According to Census 2017 the total population of Mirpur district was approximately 456,200. Geologically, the study area is seismically active. Mirpur experiences a humid subtropical climate. The annual average temperature is about 25°C and 1,380mm of rain.
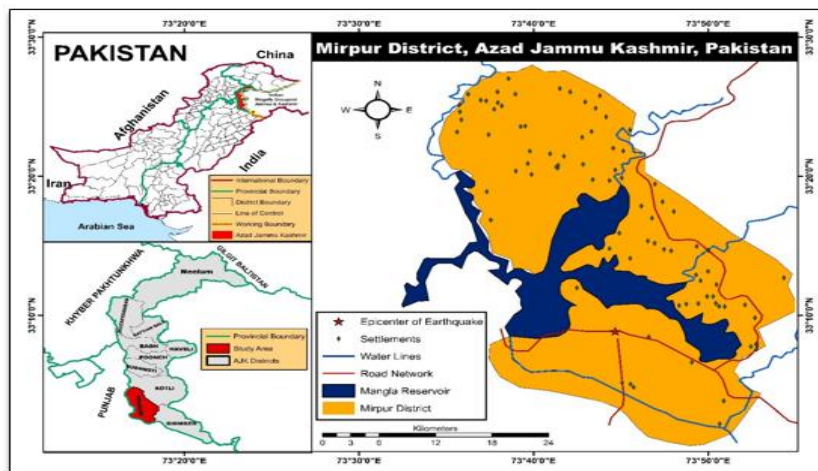
Figure 1. Location of study area

3. Research methods

For this research, data were acquired from secondary sources like National Disaster Management Authority (NDMA), Provincial Disaster Management Authority (PDMA), and satellite images. Damage data were geo-coded and then geo-visualized. The results were represented in the form of tables, graphs, and maps. Landsat Satellite data was downloaded from the open-source United State Geological Survey (USGS) open-source database (Table 1).

Table 1. Characteristics of Landsat Data (USGS, 2023)

Sr. No	Images	Year	Month
1	LANDSAT-8	2019	September
Attributes of used Bands:			
Bands	**Wavelength (micrometers)**	**Resolution (m)**	
Band 1 - Coastal aerosol	0.43-0.45	30	
Band 2 - Blue	0.45-0.51	30	
Band 3 - Green	0.53-0.59	30	
Band 4 - Red	0.64-0.67	30	
Band 5 - Near Infrared (NIR)	0.85-0.88	30	
Band 6 - Shortwave Infrared (SWIR) 1	1.57-1.65	30	
Band 7 - Shortwave Infrared (SWIR) 2	2.11-2.29	30	
Band 8 - Panchromatic	0.50-0.68	15	
Band 9 - Cirrus	1.36-1.38	30	
Band 10 - Thermal Infrared (TIRS) 1	10.6-11.19	100	
Band 11 - Thermal Infrared (TIRS) 2	11.50-12.51	100	

3.1. Data processing and analysis

Satellite images were processed to map land use land cover of district Mirpur using supervised classification Satellite as suggested by (Habib et al., 2020; Shafiq & Mahmood, 2022; Gull & Mahmood, 2022; Siraj et al., 2023; Saleem & Mahmood, 2023). For this purpose, ERDAS IMAGINE was used to organize, enhance, and display the images in Geographic Information System (GIS) environment (Bayo et al., 2022). The following steps were taken in the processing of the image:

The image downloaded from the geo-database of USGS was present in multiple bands. These bands had to be combined to get a single-layered image. It was done through the process of layer stacking in ERDAS IMAGINE. In this process, all the bands of the image were added and by running the layer stacking function single layered image was gathered. The next step was to clip the study area from the image. In the ERDAS IMAGINE, vector data was added in the form of a shape file of district Mirpur. Then, the function of the Subset was applied to the image as well as the .shp file to clip the study area.

After extracting the study area, the next step was to do supervised classification. It was done in ERDAS IMAGINE. Supervised classification was used to analyze the digital image. The pixels in the image were specified with different values to make a class of the image to analyze according to the required need of the study. It was done by clicking the RASTER tab in ERDAS IMAGINE. And clicked the SUPERVISED classification option. There appeared, a signature editor. By clicking it, the signature editor's file popped up on the screen. This signature file was used to add multiple pixels with different shades by employing drawing tools. Four classes were added under the names of Built-up, vegetation cover, barren land, and water body. Colors were assigned to the field names accordingly. Then after saving the signature file, the function of supervised classification was rubbed by clicking the supervised classification option in the raster tab. The output image was saved for processing in other software. ArcGIS 10.5 was used to work with maps and geospatial data.

Google Earth is used for the accuracy assessment of classified images. The supervised classified image was opened in ArcGIS. To calculate the area of all fields, the raster was converted into a shape file using the conversion tool in Data Management Toolbox. Then every field was selected through the selection by attributes function. In the whole process after the conversion from raster to polygon and the area of each class is calculated using an attribute table in the GIS environment.

3.2. Economic loss estimation

The estimates were based on the book value of the assets. The economic loss in various affected sectors like housing, infrastructure, and agriculture was calculated using data from concerned Department's and Authorities' websites like Livestock Census of Pakistan, Agricultural Statistics of Pakistan etc.

4. Results and discussion

A moderate earthquake of magnitude Mw 5.6 struck the Mirpur and Bhimber districts in Azad Jammu and Kashmir (AJK) Pakistan on September 24th, 2019, at 16:02 local time, causing severe damage to human life, buildings, and infrastructure. The USGS declared it a shallow earthquake.

4.1. Loss of human life

Children and women have suffered significant consequences. Table 2 shows that there were 725 total injuries, 160 of which required immediate medical attention, and 38 individuals died, of whom 34 were from the Mirpur District and 4 were from Bhimber.

Table 2. Human life loss in the study area (NDMA, 2019)

Districts	Deaths	Injuries
Bhimber	4	14
Mirpur	34	711
Total	38	725

4.2. Damages to Infrastructure

The second most terrible and unpleasant direct effect that counts a lot is the breakdown of the infrastructure. Buildings, roads, bridges, and transmission lines were all directly impacted by this earthquake. The major area in a 14km radius was impacted severely (Figure 2).
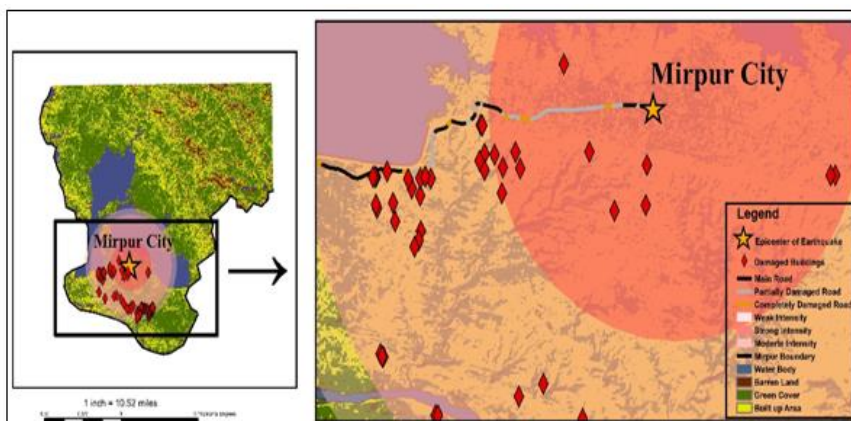

Figure 2. Spatial distribution of damages to infrastructure

Houses, workplaces, and other physical infrastructure were adversely impacted. The completely damaged (1756) and partially damaged houses (5709) in the Mirpur District. Shankikri; a village on the outskirts of Mirpur, all houses (400) were destroyed. Table 3 shows the damage to dwellings, which are divided into entirely and partially damaged entities, including residential, public, and private buildings.

Table 3. District-wise damages to buildings

Districts	Houses		Private / Govt. Buildings	
	*CD	**PD	CD	PD
Bhimber	-	4	-	-
Mirpur	1,756	5,709	9	132
Total	7,469		141	

*Completely Damaged (CD), **Partially Damaged (PD)*

Land communications, another essential component of infrastructure, were also damaged. Parts of several roads were also reportedly damaged, including two bridges. The main route between Mangla and Jatlan sustained substantial damage. Two kilometers (Km) of the road leading to Jatlan town were damaged, while 14 km of the road leading from Kharri Shareef to Jaltan was wrecked. In most places in Mirpurr and Jaltan, power cables were also disrupted. The Mangla Dam powerhouse was closed, which cost Pakistan's national power grid 900 Mega Watts (MW). At 7:20 pm, Mangla's power generation started up again, adding 700MW to the national grid. The Upper Jhelum Canal had started to develop fissures and cracks. In Jatlan town's Chak Nigah settlement, floodwaters had made it in. Later, as a precaution, the canal was closed.

The estimated economic damage generated by Completely Damaged (CD), Partially Damaged (PD) public and private buildings is highest followed by residential buildings and then roads and bridges (Table 4). The total economic loss caused by the damage is 1130 million PKR in district Mirpur.

Table 4. Total estimated economic loss in Mirpur (million PKR) (NDMA, 2019)

Sectors	Houses		*Buildings*		Cattles	Bridges	Total Estimated Economic Loss
	C.D.	P.D.	C.D.	P.D.			
Number	512	4044	9	312	580	8	
Estimated Economic loss	138	230	85	412	140	125	**1130**

4.3. Earthquake risk reduction

Pakistan has experienced different disasters in the past two decades. The social, economic, and physical infrastructure is badly affected by disasters. The risk of hydro-meteorological and geological disasters is still high because of the climatic conditions and geological settings. Therefore, it is essential to devise and practice methods to reduce disaster risks. There is a need for an earthquake risk reduction plan. Seismic risk zonation is highly required. Then zone-specific earthquake risk reduction plan needs to be prepared. The construction of earthquake resilient buildings should be encouraged. It is crucial to focus on research for seismic risk analysis at regional and national levels to increase the coping capacity of this vulnerable region. The relief activities should be planned as a risk-reduction strategy. Table 5 represents the relief provided by different authorities, departments, organizations, and agencies but still, there were deficiencies. Relief activities should be planned based on hazard spatial extent, exposure, and risk.

Table 5. Relief provided by various government and non-governmental agencies

Items	Departments								Total	Deficient
	NDMA	SDMA	DDMA Mirpur	PDMA KP	PDMA PB	Army	PRCS	NGOs		
Tents	4500	480	100	200	1000	2644	-	300	**9932444**	**3500**
Blankets	590	200	200	400	-	4500	-	-	**11200**	**7000**
Ration Packs (Kg)	1300	-	-	-	3500	-	500	175	**5676**	**6000**
First Aid Kits	200	-	-	-	-	-	-	-	**200**	**500**
Water Bottles (Liters)	50000	-	-	-	-	4300	-	6000	**60,300**	**40,000**
Kitchen Sets	275	-	-	200	-	-	-	-	**475**	**500**
Generators	-	5	1	-	-	-	-	-	**6**	**4**
Plastic Mats	-	200	60	-	-	-	-	-	**260**	**500**

5. Conclusion

A disaster such as an earthquake has the potential to significantly harm the environment, buildings, and structures yet resulting in a significant number of fatalities. As a result, disaster relief and rescue authorities must evaluate the damage for the purpose of planning. This paper assesses the post-earthquake damage that occurred in Mirpur on 2019-September. The study concludes that Mirpur is in a seismically active region where earthquakes are frequent leading to human life loss and damage to property and infrastructure. An earthquake of magnitude Mw 5.6 struck the Mirpur and Bhimber districts in Azad Jammu and Kashmir (AJK) Pakistan on September 24th, 2019, caused severe damage to human life, buildings, and infrastructure. Mirpur city, Jatlan town, and Manda and Afzalpur villages were the most affected areas. The findings revealed that road and housing damage is significant in proximity to the Mangla Dam. According to the analysis, shallow earthquakes with high magnitudes can have catastrophic impacts. Additionally, it increases the possibility of Dam Lake Outburst Flooding (DLOF), which may severely damage areas downriver. The estimated economic loss caused by damage to buildings was the highest followed by infrastructure, particularly roads and bridges. The total estimated economic loss was 1130 million PKR in district Mirpur.

An earthquake risk reduction plan is highly required to reduce human losses, economic losses, and physical damage. District Disaster Management Authority should capacitate for quick response in emergencies. Evacuation plans and community training are highly required. Land use planning and management, and implementation of building codes are also the need of time to reduce the risk of potential damage.

Author Contributions

Warda Habib: Literature review, field study. **Shakeel Mahmood:** Conceptualization, methodology, original-draft, supervision. **Noor ul Huda:** Literature review, investigation. **Siddra Noor:** Methodology, literature review. **Arslan Saleem:** Conceptualization, literature review. **Muhammad Siraj:** Literature review, investigation. **Haseeb Ahmad:** Investigation, field study.

Statement of Conflicts of Interest

There is no conflict of interest.

Statement of Research and Publication Ethics

Research and publication ethics were complied with in the study.

References

Ahmed, J., Shah, M., Awais, M., Jin, S., Zafar, W. A., Ahmad, N., Amin, A., Shah, M. A., & Ali, I. (2022). Seismo-ionospheric anomalies before the 2019 Mirpur earthquake from ionosonde measurements. *Advances in Space Research*, 69(1), 26-34. https://doi.org/10.1016/j.asr.2021.07.030

Ainuddin, S., Mukhtar, M., & Ainuddin, S. (2014). Public perception about enforcement of building codes as a risk reduction strategy for seismic safety in Quetta, Baluchistan. *International Journal for Disaster Risk Reduction,* 9, 99-106. https://doi.org/10.1016/j.ijdrr.2014.04.007

Bayo, B., Habib, W., & Mahmood, S. (2022). Spatio-temporal assessment of mangrove cover in the Gambia using combined mangrove recognition index. *Advanced Remote Sensing*, 2(2), 74-84.

Çelik, M. Ö., & Yakar, M. (2023). Monitoring land use and land cover change using remote sensing and GIS: A case study in Mersin, Türkiye. *Turkish Journal of Geographic Information Systems,* 5(1), 43-51. https://doi.org/10.56130/tucbis.1300704

Gardezi, S. A. H., Hussain, G., Neupane, B., Imran, M., Hamid, Q. Y., Ikram, N., Usmani, N. A., & Asghar, H. (2021). Geological investigation of 5.6 MW Mirpur earthquake, northwestern Himalayas, Pakistan. *International Research Journal of Earth Sciences*, 9(1), 20-31.

Gull, A., & Mahmood, S. (2022). Spatio-temporal analysis and trend prediction of land cover changes using the markov chain model in Islamabad, Pakistan. *Advanced GIS,* 2(2), 52-62.

Habib, W., Aslam, R. W., Akram, M. A. N., Khalid, M. B., Abbas, W., Tahir, M. H., Ullah, H., Mehmood, H., & Mirza, A. I. (2020). Assessment of temporal changes in landuse patterns by incorporating topographical parameters. *International Journal of Sustainable Development*, 2, 99-113

Hidayat, R. F., Kiyota, T., Tada, N., Hayakawa, J., & Nawir, H. (2020). Reconnaissance on liquefaction-induced flow failure caused by the 2018 M W 7.5 Sulawesi earthquake, Palu, Indonesia. *Journal of Engineering and Technological Sciences*, 52(1), 51-65.

Idris, Y., Cummins, P., Rusydy, I., Muksin, U., Syamsidik, Habibie, M. Y., & Meilianda, E. (2022). Post-earthquake damage assessment after the 6.5 mw earthquake on December 7th, 2016, in Pidie Jaya, Indonesia. *Journal of Earthquake Engineering*, 26(1), 409-426. Post-earthquake damage assessment after the 6.5 mw earthquake on December 7th, 2016, in Pidie Jaya, Indonesia. https://doi.org/10.1080/13632469.2019.1689868

Kencanawati, N. N., Agustawijaya, D. S., & Taruna, R. M. (2020). An Investigation of building seismic design parameters in Mataram city using Lombok earthquake 2018 ground motion. *Journal of Engineering & Technological Sciences,* 52(5). https://doi.org/10.5614/j.eng.technol.sci.2020.52.5.4

Khan, M. M. J. (2021). Capacity need assessment for earthquake response in Dhaka city [Doctoral thesis, University of Dhaka]. Institute of Business Administration. http://repository.library.du.ac.bd:8080/handle/123456789/1727

Khan, M. Y., Turab, S. A., Riaz, M. S., Atekwana, E. A., Muhammad, S., Butt, N. A., Abbas, S. M., Zafar, W. A., & Ohenhen, L. O. (2021). Investigation of coseismic

liquefaction-induced ground deformation associated with the 2019 Mw 5.8 Mirpur, Pakistan, earthquake using near-surface electrical resistivity tomography and geological data. *Near Surface Geophysics*, 19(2), 169-182. https://doi.org/10.1002/nsg.12148

Lallemant, D., Soden, R., Rubinyi, S., Loos, S., Barns, K., & Bhattacharjee, G. (2017). Post-disaster damage assessments as catalysts for recovery: A look at assessments conducted in the wake of the 2015 Gorkha, Nepal, earthquake. *Earthquake Spectra*, 33(1_suppl), 435-451. https://doi.org/10.1193/120316eqs222m

Mangkoesoebroto, S. P., Prayoga, M. H., & Parithusta, R. (2019). Collapse Risks of Fail-Safe RC Frames Due to Earthquakes: Fragility Assessments. *Journal of Engineering & Technological Sciences,* 51(4).

Mikhail, R., Irsyam, M., Nazir, R., Asrurifak, M., Hutapea, B.M., Rustiani, S., Munirwansyah, M., & Harninto, D.S. (2019). Development of Nationwide Surface Spectral Acceleration Maps for Earthquake Resistant Design of Bridges Based on National Hazard Maps of Indonesia 2017. *Journal of Engineering and Technological Sciences,* 51(4). https://doi.org/10.5614/j.eng.technol.sci.2019.51.4.4

NDMA. (2019) National Disaster Management Authority (NDMA) Situation Report No. 19 - Mirpur Earthquake 2019. Retrieved March 15, 2023, https://reliefweb.int/report/pakistan/ndma-situation-report-no-19-mirpur-earthquake-2019-dated-11-october-2019-1500-hours

Rafi, M. M., Ahmed, M., Lodi, S. H., Varum, H., & Arshad, M. T. (2022). Investigation of damage to Reinforced concrete buildings due to the 2019 Mirpur Earthquake, Azad Kashmir. *Journal of Performance of Constructed Facilities,* 36(5), 04022037. https://doi.org/10.1061/(ASCE)CF.1943-5509.000174

Saleem, A.., & Mahmood, S. (2023). Spatio-temporal assessment of urban growth using multi-stage satellite imageries in Faisalabad, Pakistan. *Advanced Remote Sensing,* 3(1), 10–18.

Sengara, I.W., Sidhi, I.D., Mulia, A., Asrurifak, M., & Hutabarat, D. (2016). Development of Risk Coefficient for Input to New Indonesian Seismic Building Codes. *Journal of Engineering & Technological Sciences*, 48(1). https://doi.org/10.5614/j.eng.technol.sci.2016.48.1.5

Shafiq, M., & Mahmood, S. (2022). Spatial Assessment of Forest Cover Change in Azad Kashmir, Pakistan. *Advanced GIS*, 2(2), 63-70.

Shakya, M., Kawan, C. K., Gaire, A. K., & Duwal, S. (2021). Post-earthquake damage assessment of traditional masonry buildings: A case study of Bhaktapur municipality following 2015 Gorkha (Nepal) earthquake. *Engineering Failure Analysis*, 123, 105277. https://doi.org/10.1016/j.engfailanal.2021.105277

Sidi, I.D. (2017). Probabilistic Modeling of Seismic Risk Based Design for a Dual System Structure. *Journal of Engineering & Technological Sciences,* 49(2). https://doi.org/10.5614/j.eng.technol.sci.2017.49.2.2

Siraj, M., Mahmood, S., & Habib, W. (2023). Geospatial assessment of land cover change in District Dera Ismail Khan, Khyber Pakhtunkhwa, Pakistan. *Advanced Remote Sensing*, 3(1), 1–9.

Sreejith, K. M., Jasir, M. C. M., Agrawal, R., & Rajawat, A. S. (2021). The 2019 September 24, Mw= 6, Mirpur earthquake, NW Himalaya: Geodetic evidence for shallow, near-horizontal décollement rupture of the Main Himalayan Thrust. *Tectonophysics*, 816, 229013. https://doi.org/10.1016/j.tecto.2021.229013

Stevenson, J. R., Becker, J., Cradock-Henry, N., Johal, S., Johnston, D., Orchiston, C., & Seville, E. (2017). Economic and social reconnaissance: Kaikōura earthquake 2016. *Bulletin of the New Zealand Society for Earthquake Engineering*, 50(2), 343-351. https://doi.org/10.5459/bnzsee.50.2.343-351

USGS. (2023). Belsis. (2023). United States Geological Survey, Science Technology. Retrieved June 15, 2023, from https://www.usgs.gov/faqs/what-are-band-designations-landsat-satellites

Wu, H., Ai, H., Zhou, R., Hong, Z., He, Y., & Li, J. (2022). Research on Rapid Assessment of Earthquake Disaster and Emergency Relief Material Distribution System--Case Study on Earthquake in Yangbi County, Yunnan Province, China. *Sensors & Materials*, 34.

Spatial ecological risk analysis in peach farming in Manisa

Emre Yeniay[*1] , **Aydın Şık**[2]

1Republic of Türkiye Ministry of Agriculture and Forestry General Directorate of Plant Production
2Gazi University, Architecture Faculty, Department of Industrial Design, Ankara, Türkiye

ABSTRACT

With the help of information technologies, which are developing day by day, it has become easier to perform agricultural analyzes. Positional analyses can be performed with the help of Geographical Information Systems by gathering Climate, Soil, Topography and İrrigation data related to Agriculture. These analyses enables to generate analyses for agricultural investment maps, areas of agricultural conformity, plant pattern determination, etc. The purpose of this study is to prepare "Product Based Agricultural Risk Analysis Maps". Climate, Soil, Topography and Irrigation data, which are important in the growing of agricultural products are collected, severity and prospects for risk analysis are determined separately and risk values are established for each risk factor. The total risk value was calculated by prioritizing risk factors using the Analytical Hierarchy Process (AHP), one of the multi-criteria decision-making methods. Thanks to AHP, a methodology for calculating scenario-based risk values has been developed taking into account different probabilities. With the developed model, risk maps were created for climate, soil, topography and water constraints. The total risk map was obtained by combining the risk maps created with AHP. In this study, a model was established by taking the Peach and Fig product of Manisa and as a result of the model, Total Risk values were divided into classes such as "High Risk Areas", "Medium Risk Areas", "Low Risk Areas" and "Strictly Not Recommended Areas" according to the scores they received positional.

1. Introduction

According to the latest report of the United Nations, the current world population of 7.6 billion is expected to reach 8.6 billion in 2030, 9.8 billion in 2050 and 11.2 billion in 2100. Many difficulties on agricultural supply chains, shrinking agricultural land sizes, environmental problems and the inability to protect natural resources have made it necessary to take urgent measures to meet the food needs of the increasing world population. To meet these challenges, farming systems require a major and fundamental shift from traditional practices to precision farming or smart farming practices. Geographic information system (GIS) is a useful technology that facilitates the transition from existing methods to precision agriculture. (Sharma et al., 2018).

About 13 billion hectares of the earth's surface are covered with land, of which 37 percent is agricultural lands, about 5 billion hectares. Considering the distribution of the agricultural land asset in question according to the way of use, it is seen that field crops are grown in approximately 1.5 billion hectares of land, and perennial plants are planted in 1.5 billion hectares. The

remaining 2 billion hectares are evaluated as meadows and pastures (OKP, 2013).

The strategic importance of the protection and development of agricultural production, the continuity of nutrition, which is the basic need of human beings, the supply of food raw materials and the sustainability of the agricultural industry, has become more evident especially during the COVID-19 Pandemic process. The existing agricultural areas in the world are decreasing by about 0.1-0.2% in every 5 years. On the other hand, the world population has increased by about 6.2% in the last 5 years. (UN, 2013). In our country, the total amount of land cultivated between 2001 and 2020 decreased by 3 million 205 thousand hectares, from 26 million 350 thousand hectares to 23 million 145 thousand hectares. (TUIK, 2021a). The rate of decrease was realized as 12 percent. In the same period, our population increased by 18 million 219 thousand and became 83 million 385 thousand. The rate of increase is 28%. (TUIK, 2021b).

As a result, although the increasing world population increases the demand for food, decreasing agricultural areas and disasters as a result of changing climatic conditions bring along serious decreases in food supply in the opposite proportion. At this point, it seems that the way out is to switch to smart, planned and

Cite this article

Yeniay E., & Şık, A. (2023). Spatial ecological risk analysis in peach farming in Manisa. *Advanced GIS*, 3(2), 59-67.

sensitive agriculture, which is also called Agriculture 4.0, where information systems are used from traditional agricultural methods. In smart and planned agriculture, it is possible to determine from the very beginning what to grow and where, and to obtain products that are least affected by diseases and pests due to both an increase in yield and products grown under ideal conditions. However, it is not always possible to choose land with ideal conditions. At this point, knowing in advance what kind of risks the existing land has, thanks to the work done, enables the creation of artificial conditions to correct the factors that cause damage.

2. Method

Fault tree analysis (FTA) is a well-constructed, precise and powerful tool that can be used to assist the analyst in identifying, evaluating and analyzing all root causes and pathways leading up to the occurrence of a particular event. In the traditional approach, the probability of fundamental events is considered either as a definite point value or as a random time dependent variable. However, due to the inherent impreciseness and uncertainty of the available data, it is often impossible to obtain a precise estimate of the incidence or distribution function of an event. (Jafarian et al., 2012)

Events graphically described in the fault tree diagram and the factors that cause these events can be attributed to different events that cause errors, accidents, losses or undesirable results. The FTA method can be used qualitatively to identify the causes and events leading to a fault, and can also be used quantitatively to calculate the probability of recurrence of the root cause. During the design phase of a system, the FTA method is also used to calculate potential losses and sum them up from different design options, to estimate the significance of potential losses during the operation phase (Çınar, 2004). To build a tree, a final event is placed at the top and then linked to logic symbols representing the conditions for the event to occur, and then to intermediate events that cause the high event. For example, the symbol OR means that at least one intermediate event must occur for the higher event to occur, while the symbol AND means that at least two or more intermediate events must occur for the higher event to occur.

In the study, the reasons that may cause an undesirable situation are determined and analyzed based on the deductive logic. The severity of the risk arising from undesirable conditions is calculated by the FTA method. Risk factors are organized, defined and presented in a tree diagram with a logical system. Undesirable peak events are detected and any factor considered in this event should be analysed. The model setup is started by using the total risk value of a selected fruit product. As a result, sub-risks such as climate, soil, topography, water restrictions that cause total risk are determined. Factors causing sub-risks are selected on a product basis and entered into the system in layers. The risk analysis model developed with the FTA method used in complex systems focuses on the risk of only one product at a time. The layers that may cause product risk

for each product are entered separately and the total product risk maps are formed.

2.1. Dataset

Statistical and numerical data obtained from various public institutions and organizations were transferred to the geographic database created in ArcGIS 10.5 application. Transformation of statistical data into digital format has been done.

Climate data set prepared by the General Directorate of Meteorology, land cover, land use capability, current land use, soil maps prepared by the abolished general directorate of soil and water, created by the abolished Ministry of Agriculture and Rural Affairs, 1/25,000 topographic maps provided by the General Command of Mapping and irrigated land assets, streams, streams and rivers data prepared by DSI and DSI were obtained and all climate, soil, topography and water asset maps were standardized by making projection transformations.

Climate Data: The last 30 years (1990-2020) climate data of Manisa Province were used by the General Directorate of Meteorology. These data were classified as monthly and monthly average, minimum and maximum values were calculated. Finally, statistical data obtained from meteorological observation stations with known coordinates were transformed into spatial format by applying surface spread with "co-kriging" and inverse distance weighting (IDW) methods with ArcGIS software. In the process of spreading to the surface, taking into account the topography, the values were assigned to the cells with the dimensions of 20 x 20 meters and the climate maps classified in the raster format in table 1 were created. A GIS database has been created specifically for the province.

Statistical and numerical data obtained from various public institutions and organizations were transferred to the geographic database created in ArcGIS 10.5 application. Transformation of statistical data into digital format has been done.

2.2. Risk analysis

Risk analysis is the process of identifying and analyzing potential problems that may adversely affect investment ventures or production. This process is done to help organizations prevent or mitigate these risks.

FTA is a type of defect analysis in which an undesirable condition in a manufacturing process is examined (Figure 1). This analysis method is used to understand how systems can fail, determine the best ways to mitigate risk, or determine the tolerance level of a particular system for risks. FTA is used in aerospace, nuclear power, chemical and process, pharmaceutical, petrochemical and other high-risk industries; however, it is also used in a wide variety of fields such as determining risk factors that cause yield loss in agricultural production (Tuncay, 2017).

Table 1. GIS datasets

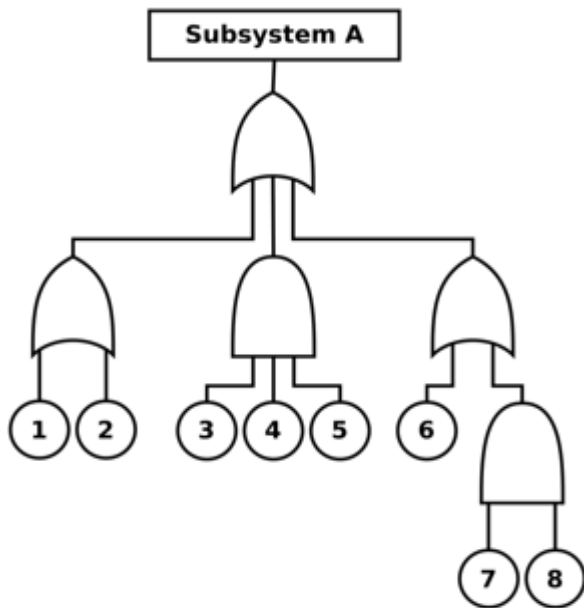|		Temperature		Soil Depth
Climate Data		Average Temperature on a Monthly	Soil Data	Uthosolic
		Maximum Temperature on a Monthly		Very Shallow (0-30cm)
		Minimum Temperature on a Monthly		Shallow (30-50cm)
		Extreme Maximum Temperature on a Monthly		Medium Deep (50-90cm)
		Extreme Minimum mum Temperature on a Monthly		Deep (90-150m)
		Precipitation		Very Deep (>150cm)
		Total Precipitation on a Monthly		**Soil Erosion**
		Summer Months Total Precipitation		Wind Erosion
		Total Annual Precipitation		**Rain Erosion**
		Sunbathing		**Land Use Capability**
		Total Sunbathing Times on a Monthly		1-8th Class Land
		Total Annual Sunbathing Times		**Available Land Use**
		Evaporation		Absolute Irrigated Farmland
		Evaporation Values on a Monthly		Marginal Irrigated Farmland
		Average Annual Amount		Absolutely Dry Farmland
		Humidity		Marginal Dry Farmland
		Average Humidity Values on a Monthly		Planted Agricultural Land
		Spring Months Average Humidity Value		Meadowland Pasture Areas
		Wind		Wetlands
		Average Wind Speed on a Monthly		Forest Areas
		Soil Temperature		More Fields
Water Data		Irrigation		**Drainage**
		Streams	Topography Data	Height
		Dams and Lakes		Slope
				Aspect

Figure 1. A fault tree diagram

In agriculture, the more general term "yield loss" is used for the "failure" / top event of the fault tree. These conditions are classified according to the severity of their effects. The most severe environmental conditions require the most comprehensive fault tree analysis in which ecological factors are examined in detail. These yield loss conditions and their classification are often predetermined in the hazard analysis by the effects of factors such as climate, soil, topography and irrigation.

2.3. Agricultural risk analysis

FTA is a tool that can be used to help the analyst identify, evaluate, and analyze all root causes and pathways leading up to the occurrence of a particular event (Jafarian et al., 2012).

To construct a tree, a top event is placed at the top and then connected to logic symbols representing the conditions for the event to occur, and then connected to the intermediate events that caused the top event. (WHO, 2011).

The risks faced by farmers are grouped under two headings: ecological risks arising from natural events and economic risks arising from financial conditions. Today, risks such as increasing disasters (drought, hurricane, flood, frost, and hail), change of seasons, erosion, diseases and pests due to climate change are grouped under the title of ecological risks. In a recent study, researchers estimated that 23% of field crops were lost due to adverse weather conditions. In horticultural crops, this rate increases remarkably (Islam et al., 2018).

In this study, spatial risk analysis was performed with a model developed in GIS on the determination of ecological risks in fruit growing. The process proceeds in three steps. The first step is to establish the model with the FTA method, the second step is to enter the intensities and probabilities of the causes, and the third and last step is to run the model developed on the ArcGIS software and create the maps.

In the climate, soil, topography and water presence layers, the values that may pose a risk during the growth of the plant and value of the severity and probability this risk are entered. Suitable areas where a selected plant grows with high yield, that is, with the least risk, will

receive the lowest score, while areas where the growing conditions for the plant are unfavorable and contain high risk will receive the highest score in the risk matrix (Altay et al., 2018).

In addition, by assigning values between these layers according to their importance, the risk scores from the layers can be re-scored hierarchically thanks to the Weighted Overlay Analysis tool (Ahmed et al., 2013).

First of all, the process begins with the collection of data and recording it on the database after standardization. Then, the risks that may cause yield loss for each product and the probability and severity values of these risks should be determined. AHP priority values created for each sub-risk value of the risk analysis will be determined. Finally, the final total risk map will be created by combining all sub-risk layers according to hierarchical ranking and scoring according to the fault tree logic in figure 2 (Yeniay et al., 2022).

The Risk Matrix was created in table 2 using the formula "Risk= Severity x Probability (Probability)". According to the scores they got after the entered values;
•   Green areas: 1-6 low risk (1 pointless risk)
•   Yellow areas: 6 -12 medium risk
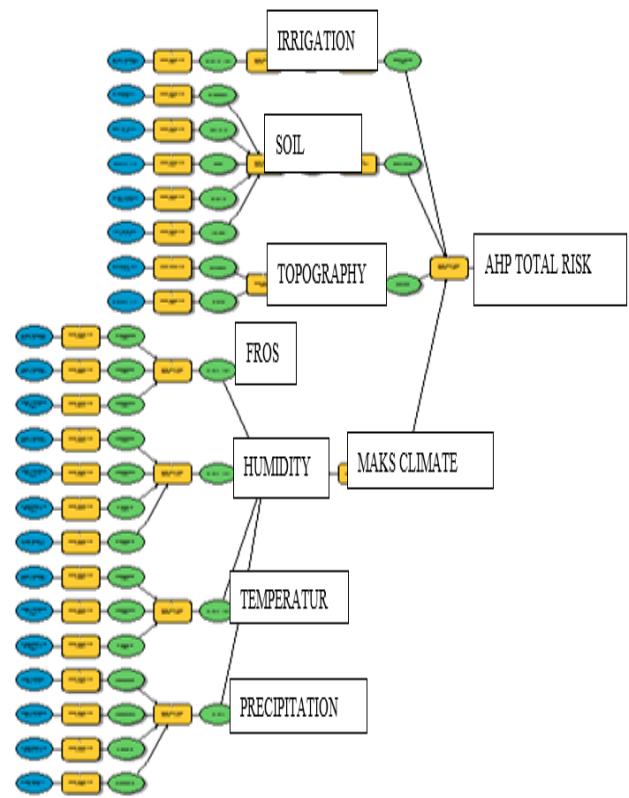•   Red areas: 12-25 are determined as high risk (25 irreparable risk).

Figure 2. GIS model fault tree

Table 2. Risk matrix

Matrix	Severity				
Probability	Very Light 1	Light 2	Moderate 3	Serious 4	Very Serious 5
Very Small 1	Meanless 1	Low 2	Low 3	Low 4	Low 5
Small 2	Low 2	Low 4	Low 6	Medium 8	Medium 10
Medium 3	Low 3	Low 6	Medium 9	Medium 12	High 15
High 4	Low 4	Medium 8	Medium 12	High 16	High 20
Too High5	Low 5	Medium 10	High 15	High 20	Irreparable 25

The GIS model assigns the probability values entered for the layers as values into each cell spatially. The average temperature value of a point selected as an example in Manisa in April is -1 °C and the severity of frost damage to the peach trees at this point is moderate 3. The average temperature value of the same point is -5 °C in March and +3 °C in May. Therefore, the average

temperature value in March and May will be 4 and 1 frost severity. However, considering the blooming periods of the peach trees at the chosen point, the probability of frost in April, when the flowering is the highest, is 5, and the probability of frost is 3 and 1 due to the low flowering in March and May (Öztekin et al,, 2008; Gür et al., 2011, Eroğlu et al, 2012.).

Table 3. Risk factors

Selected Point Layers	Temperature	Severity	Probabilities	Risk Severity	Frost Risk Factor
March	-5 °C	Serious 4	Medium 3	4x3 12	Maximum Risk Severity 15
April	-1 °C	Moderate 3	Too High 5	3x5 15	
May	+3 °C	Very Light 1	Small 1	1x2 1	

For this reason, for each risk factor, a sample table is filled as in table 3 and a "Significance Evaluation" is made by using the AHP over the risk factors. AHP is used to prioritize risk factors among risk factors. This is done with the "Weighted Overlay" analysis tool in GIS.

After the criteria and sub-criteria are determined by using the Super Decision program, the criteria that affect each other can be determined by analyzing the interactions between the criteria, and the network

structure in figure 3 is created by making connections between the criteria, internal and external dependencies, and feedbacks with the help of the program (Yeniay et al., 2022, El-Sheikh, 2010).
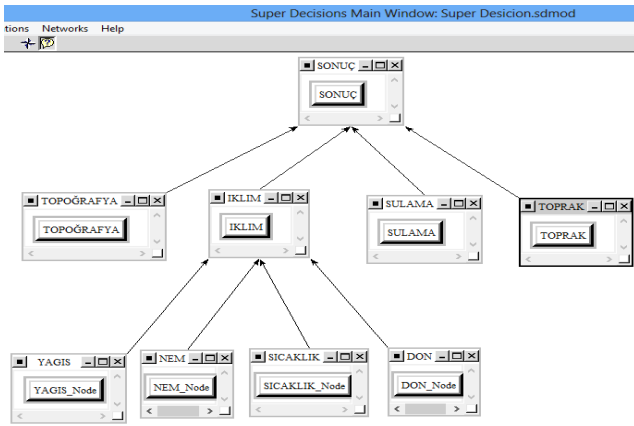
Figure 3. Super decision program interface

After entering the risk probability and severity values of all layers under the climate, soil, topography and irrigation layer groups for the peach crop, the "superiority" importance scores among the risk factors are entered in table 4 (Yeniay et al., 2022, Chuong, 2008).

Table 4. Total risk superiority table

Risk Factors			Severity Weight	Total Risk
Irrigation			0.10303	
Soil			0.11887	
Topography			0.29271	
	Layers	**Climate Max Risk**		**Climate+Topography+Soil+Irrigation =1**
Climate	Frost Humidity Temperature Precipitation	Max (Frost, Humidity, Temperature, Precipitation)	0.4809	

After this stage, risk factors ranging from 0 to 25 values were obtained in each group. "AHP priority values" between climate, soil, topography and irrigation layers are entered in the "weighted overlay" tool in GIS. Since the sum of the values entered in the AHP is equal to the full value of "1", the final values will be "total risk" values between 0 and 25. In the peach sample, the "frost risk factor" took a value of 15 at a selected point. Again, the same point took the values of "humidity", "temperature", "precipitation" 10, 12, 8 by manual calculation (Equation 1). While calculating the climate risk factor, the value of 15, which is the maximum risk among the subgroups, was taken as shown in table 3 (Mokarram et al., 2011, Nyeko 2012).

$$Climate\ Risk\ Factor = Maximum\ [Frost\ Risk, Humidity\ Risk, Precipitation\ Risk, Temperature\ Risk] \qquad (1)$$
$$Climate\ Risk\ Factor = Maksimum[\ 15, 10, 12, 8] = 15]$$

Again, in the manual calculations made for the same point, the soil took the risk value of 8, the topography 12, and the irrigation 18 risk value. The final ecological risk value was calculated by entering the prioritization scores for climate, soil, topography and irrigation with AHP (Equation 2).

$$Final\ Risk\ = Climate\ x\ 0,48\ +\ Soil\ x\ 0,12\ +\ Topography\ x\ 0,30\ +\ Irrigation\ x\ 0,10 \qquad (2)$$
$$Final\ Risk\ = 15\ x\ 0,48\ +\ 13\ x\ 0,12\ +\ 8\ x\ 0,30\ +\ 16\ x\ 0,10\ = 12,40$$

3. Results

As a result of the process, it is seen that the point selected for the cultivation of peach crops is "moderate" in the risk matrix according to the calculations. This manual calculation for a single point was automatically performed on the GIS for millions of points and group as shown in "climate", "soil", "topography", "irrigation" separate risk maps were created for the layers.

In figure 4 climate risk map created as a result of the model, it is seen that the plain region of Manisa province is at high risk in terms of peach cultivation, while the mountainous regions are at low risk.

Figure 4. Climate risk map

Soil structure is used as the most important factor in determining agricultural areas. It is not possible to carry out agricultural activities in, rocky, lithosol (shallow azonal soils), swamp, extremely salty, desert, etc. areas. Therefore, in the GIS model, primarily non-agricultural areas were masked in the soil layer and were not included in the risk analysis.

In the figure 5 soil risk map created as a result of the model, there is no homogeneous distribution in the province of Manisa in terms of peach cultivation among the existing agricultural lands.
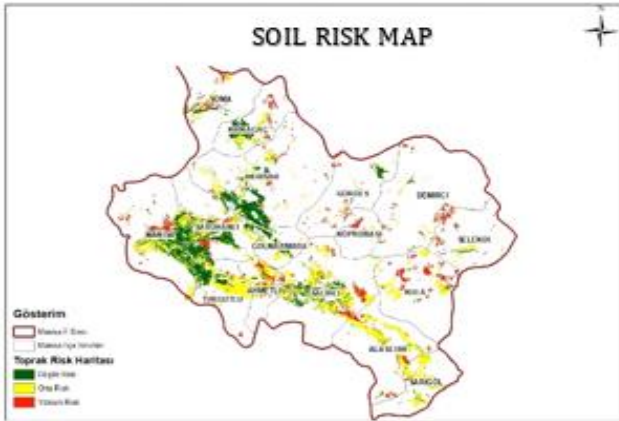

Figure 5. Soil risk map

Topography factor in fruit growing is a risk group that can be intervened more easily than other factors. With the terracing method, the minimum level of slope risk factor can be reduced. The elevation risk factor can play a role in increasing the quality of fruit growing when the climatic risks are eliminated. In Figure 7, it is seen that the low risk ratio is spread over wider areas in the topography risk map.
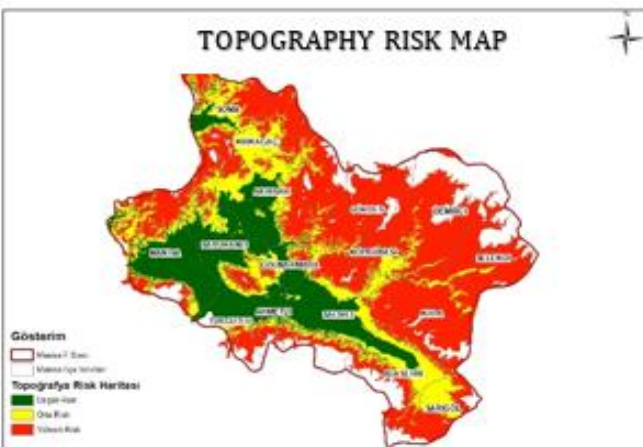

Figure 6. Topography risk map

Another important layer in fruit growing is irrigation. Peach cultivation is done in the form of irrigated agriculture. The existing public irrigation area is low risk, and other areas where individual irrigation activities can be carried out are determined as high risk in the irrigation risk map in figure 7.

Figure 7. Irrigation risk map

The negative impact of each sub-risk factor on crop yield is different. Therefore, the effect of the sub-risk factor on the total risk will be different according to the AHP priority value. The final risk map of the peach crop in figure 8 was obtained by combining the climate, soil, topography and irrigation sub-risks as a result of hierarchical scoring.
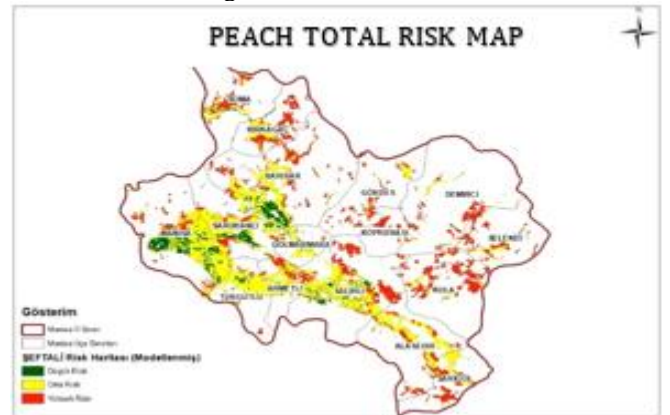

Figure 8. Peach total risk maps in Manisa, Türkiye

In table 5, TUIK 2020 plant production statistics are given for the peach product in Manisa Province. According to TUIK 2020 data, the maximum peach yield in Turkey is 85 kg per tree, and the average yield is 49 kg. It is understood that the average yield of peach products in all other districts of Manisa, except Şehzadeler (Center), Turgutlu and Sarıgöl districts, is below the country average. It is seen that the yield is quite low in direct proportion to the statistics in the high-risk red areas on the map, while the yield is relatively high in the low-risk green areas.

Most of the Manisa Plain appears to be medium risk. When the sub-risk factors are examined, the plain region seems to be low risk in soil, topography and irrigation layers, but climatic factors, which are the main limiting factors in fruit growing, resulted in high risk in the plain. It is seen that the climate risk factor is of high importance and the total risk factor also affects it in that direction.

Table 5. TUIK 2020 plant production statistics (Manisa province, peach product)

Manisa Peach	Number of Trees	Yield (Kg/Tree)	Production Amount (Ton)
Ahmetli	1.875	30	56
Akhisar	4.000	32	128
Alaşehir	12.550	30	377
Demirci	1.160	17	20
Gölmarmara	1.350	22	30
Gördes	6.750	12	81
Kula	1.901	20	38
Köprübaşı	1.450	15	22
Kırkağaç	7.530	24	181
Salihli	19.880	30	596
Saruhanlı	1.670	20	33
Sarıgöl	20.400	61	1.244
Selendi	2.740	30	82
Soma	3.100	20	62
Turgutlu	180.320	50	9.016
Yunusemre	900	20	18
Manisa (Şehzadeler)	80.000	60	4.800

4. Discussion

In this study, it is aimed to create product risk maps that aim to maximize the amount of product obtained from limited resources by being affected by less risks thanks to the developing information technologies in agricultural production. In the researches, it is understood that the biggest problem of the current century is agricultural disasters and harvest losses as a result of the devastating effects of climate change, in addition to the food security hazard to be caused by the increasing population and decreasing agricultural lands. In the COVID-19 pandemic period we are in, the need to develop policies for the protection of food safety on a global scale has made agriculture a strategic sector like never before. Despite this, many innovations brought by today's technologies provide many advantages in terms of ensuring food safety. Therefore, instead of ancestral methods, it has become a necessity to use precision agriculture techniques, also called agriculture 4.0, by taking advantage of the opportunities of developing technology, where all stages of agriculture are recorded and as a result, we will obtain a more predictable harvest (Gitz et al., 2016, Pablo et al., 2014).

Geographical information systems (GIS), on the other hand, is an information platform where location-based analyzes can be made. Since agriculture is a sector based on location and data, it is among the areas where GIS examples are most commonly used. With GIS, various simulations can be made by using the data produced based on observations, records and predictions for many years. In this study, simulations were made with modeling methods using climate, soil, topography and irrigation data produced for many years at this point. Of course, the biggest factor determining the accuracy of the study is the accuracy rate of the data used. One hundred percent correct preparation will be so accurate in the results obtained with soil maps, climate data and irrigation data. Knowing that the basis of the data used in the study dates back to the previous century is a question mark in terms of the reliability of the results of the study.

However, no contradiction was encountered in the results obtained with statistical validations. (SDÜ, 2020)

When risk analysis methods are examined, it is evaluated that methods and theorems developed for the complex industry sector and accepted in international platforms will be valid in agriculture. Based on this, the risks that may cause yield loss in fruit growing were determined by entering the fault tree matrix, which is the most common method in risk analysis. With the deductive method, the main factors causing yield loss were determined as climate, soil, topography and irrigation, and a fault tree was formed by determining the sub-factors determining these main factors. The GIS data of each risk factor in the fault tree were obtained from the relevant institutions and organizations statistically, such as meteorological data, and converted into GIS format by spreading over the surface with IDW, Kriking and Ko-Kriking methods, and already provided in GIS format such as soil, topography and irrigation data. .

After creating a geographic database from all GIS data and determining the risks that cause loss of productivity, it has come to the stage of creating the information about the risk area model institution and which risk will affect the severity and probability of the loss of efficiency. Here, however, there are some uncertainties such as the type, type and variety of the fruit grown. Because it is a creature that lives in fruit, and just like humans, it may have experienced different adaptations in different ecological conditions. However, since it is not possible to proceed with this uncertainty, the data needed for the model is entered based on the general ecological demands of the most common fruit varieties produced and cultivated for commercial purposes. Ecological demands were determined as a result of studies in which a plant's growing conditions were observed in the most suitable conditions with the highest efficiency. In addition, adverse climatic conditions that occurred over the years and caused yield loss were recorded as marginal conditions.

The ecological conditions with the highest yield were determined as the lowest score in terms of risk severity, and the marginal conditions causing yield loss were determined as the highest score according to the risk severity degree. The risk probability value was determined by considering the developmental physiology of the plant on a monthly basis under climatic conditions. In the soil, topography and irrigation risk layers, the probability values were determined according to the probability of affecting the yield among the lower layers of each layer the most.

Finally, since the risk factors coming from the climate, soil and topography risk layers cannot cause equal yield loss, prioritization between the layers was made with the Analytical Hierarchy Process (AHP) method and the total risk value was obtained for millions of points with a size of 20x20 square meters. The risk values at these millions of points were classified according to the values in the risk matrix on the GIS and separate risk maps were obtained for each product.

First of all, producers who want to establish new gardens can choose the land using these risk maps and achieve the highest production by experiencing minimum yield loss in the lowest risk lands. Of course,

production in low-risk regions will reduce input costs, increase profitability and contribute to more natural and healthy production in the decrease in fertilizers, pesticides and agricultural structures.

As a result of the risk map examinations to be made, it will be possible to determine the existing risks in the orchards that have already been established. It will be possible to see from which factors the risks created by the fault tree originate in the lower layers. In this way, there will be an opportunity to take precautions since the factors that may cause loss of efficiency are known in advance. Thanks to meteorological early warning systems, some small cost measures that can be taken for previously known risks will result in a significant increase in efficiency (Yeniay et al., 2022).

According to the 2020 data of the Turkish Statistical Institute, the maximum peach yield per tree in Turkey is 85 kg, and the average yield is 49 kg. According to the same data, peach yield is high in Manisa Province Center, Saruhanlı, Akhisar, Turgutlu, Salihli and Sarıgöl districts. In the high-risk red areas in the risk map created as a result of the model, the yield is low in direct proportion to the statistics, while the yield is high in the low-risk green areas. Most of the Manisa Plain appears to be medium risk. When the sub-risk factors are examined, the plain region seems to be low risk in soil, topography and irrigation layers, but climatic factors, which are the main limiting factors in fruit growing, resulted in high risk in the plain.

5. Conclusion

The developed model can be revised on a product-based basis, in the light of more reliable data using more precise ecological demands for each product type. In the commercial use of products registered as certified saplings, maps showing the areas where seedlings can be grown can be given to the producer. It is even possible to give a specific variety recommendation for the producer's parcel. In this way, maximum benefit can be obtained from limited areas by switching to a planned production.

Using the created model, risk analysis maps were created for the province of Manisa. Peach and fig products were selected as examples in Manisa. The peach product in Manisa is among the provinces where the most cultivated crops are grown in Turkey. In addition, due to ecological factors, many fruit products are grown in Manisa with high yield.

Separate risk maps were drawn for climate, soil, topography and irrigation factors for two crops. After prioritizing all layers with the fault tree method and AHP, a total risk map of the peach product was created. Thanks to the defect tree analysis, it is possible to easily access the sub-risks that cause the main yield loss of the peach product, with a retrospective analysis.

When the peach risk map is examined in detail; It has been determined that the peach crop is more sensitive to climatic and soil conditions and is highly affected by the risk factors coming from the climate and topography layers. There are large plains throughout the province of Manisa. Although the topography risk is low in the plain region, the risk is higher in the transitional regions. There are large and fertile plains in Manisa province. This plain area is not considered as a serious risk in terms of soil and irrigation. However, in the months when windless and high temperatures are experienced, climatic risks against diseases and pests increase. In addition, areas with high climatic risks have been identified in some transition regions. It has been concluded that total peach risk factors can be improved with cultural and mechanical climatic improvements. Thanks to such improvements, healthier products will be obtained as there will be less disease fighting. As a result of the digitization of the maps, a total of 2,145,219 decares of land can be grown in peach, and 274,626 decares of these areas are low risk, 1,199,908 decares are medium risk, and 670,684 decares are high risk.

It has been determined that the fig crop is less sensitive to soil conditions and is highly affected by the risk factors coming from the climatic layers. In total, crops can be grown in 2,840,771 decares, and 1,256,186 decares of these areas are low risk, 1,561,777 decares are medium risk, and 32,813 decares are high risk. According to these results, peach product can be affected by risk factors in wider narrow areas and risk factors compared to figs, while fig product can be grown in wider areas with low risk. It is considered that the main risk factor in the cultivation of peach crops in Manisa is late spring frosts.

Considering the climate, soil, topography and irrigation data throughout Turkey, a site selection analysis can be made for all plant products with known ecological demands by using the developed model in this study. . After examining the risk maps, a methodology study can be carried out to find answers to the questions of which crops may grow more risky in various regions and which of these risks are caused by climate, soil, topography and irrigation factors, and finally, what measures can be taken against them can be easily determined with the help of fault tree analysis.

Author Contributions

Author1: Methodology, software, data curation, Writing-Original draft preparation, validation, visualization, **Author2:** Reviewing, editing.

Statement of Conflicts of Interest

There is no conflict of interest between the authors.

Statement of Research and Publication Ethics

Research and publication ethics were complied with in the study.

References

Ahmed, H. R., & Terribile, F. (2013). İntroducing a new parametric concept for land suitability assessment. İnternational. *Journal of Environmental Science and Development,* 4(1), 15-19. https://doi.org/10.7763/ıjesd.2013.v4.295

Altay, Y., & Keskin, İ. (2018). Determination of factors affecting wheat production in altınekin district by risk analysis. *Selcuk Journal of Agriculture and Food Sciences,* 32(3), 496-501. https://doi.org/10.15316/SJAFS.2018.128

Chuong, H. V. (2008). Multicriteria land suitability evaluation for crops using gis at the community level in central vietnam. *International Symposium On Geoinformatics For Spatial Infrastructure Development In Earth And Allied Sciences*, Hanoi, Vietnam.

Çınar, Y. (2004). *Multi attribute decision making and an implementation on evaluation of financial performances of banks* Publication No. 141376) [Master's Thesis, Ankara University]. YÖK National Thesis Center.

El-Sheikh, R. F. A., Ahmad, N., N. Shariff, A. R. M., Balasundram, S. K., & Yahaya, S. (2010). An agricultural investment map based on geographic information system and multi-criteria method. *Journal of Applied Sciences,* 10(15), 1596-1602. https://doi.org/10.3923/jas.2010.1596.1602

Eroğlu, Ö. Z., & Mısırlı, A. (2012). Şeftali ıslahı ve gelişimi. *Bahçe,* 41(2), 37-46.

Gitz, V., A. Meybeck, L. Lipper, C. D. Young, & Braatz, S. (2016). Climate change and food security: risks and responses. *Food And Agriculture Organization Of The United Nations (FAO),* 110, 2-4.

Gür, İ., & Pırlak, L. (2011). Determination of phenological and pomological characters of some peach cultivars grown in Egirdir ecological conditions. *Batı Akdeniz Tarımsal Araştırma Enstitüsü Derim Dergisi (in Turkish)*, 28(2), 27-41.

Islam, M. M., Ahamed, T., & Noguchi, R. (2018). Land suitability and ınsurance premiums: a GIS-based multi-criteria analysis approach for sustainable rice production. *Sustainability*, 10(6), 1759. https://doi.org/10.3390/su10061759

Jafarian, E., & Rezvani, M. A. (2012). Application of fuzzy fault tree analysis for evaluation of railway safety risks: an evaluation of root causes for passenger train derailment. *Proceedings of the Institution of Mechanical Engineers, Part F: Journal of Rail and Rapid Transit,* 226(1), 14-25. https://doi.org/10.1177/0954409711403678

Mokarram, M., S. A., Marnani, A. A., Moezi, & Hamzeh, S. (2011). Land suitability evaluation using ordered weight averaging with fuzzy quantifier in Shavoor plain, Iran. *Research on Crops*, 12(2), 593-599.

Nyeko, M. (2012). GIS and multi-criteria decision analysis for land use resource planning. *Journal of Geographic Information System,* 4(04), 341-348. https://doi.org/10.4236/jgis.2012.44039

OKP. (2013). *Türkiye Cumhuriyeti Kalkınma Bakanlığı Onuncu Kalkınma Planı (2014-2018) in Turkish.* Retrieved January 29, 2023, from https://www.sbb.gov.tr/wp-content/uploads/2022/08/Onuncu_Kalkinma_Plani-2014-2018.pdf

Öztekin, T., Susam, T., & Gerçekçioğlu, R. (2008). Determination the appropriateness of Tokat Kazova lands to peach cultivation using geographic information system. *Journal of Tekirdag Agricultural Faculty,* 5(2), 215-225.

Pablo J., Hubbard, N., & Loudjani, P. (2014). *Precision Agriculture: An Opportunıty For Eu Farmers - Potential Support With The Cap 2014-2020.* Directorate-General For Internal Policies, Agriculture And Rural Development, European Parlement. Retrieved January 29, 2023, from https://Www.Europarl.Europa.Eu/Regdata/Etudes/Note/Join/2014/529049/İpol-Agri_Nt(2014)529049_En.Pdf

Sharma, R., Kamble, S. S., & Gunasekaran, A. (2018). Big GIS analytics framework for agriculture supply chains: A literature review identifying the current trends and future perspectives. *Computers and Electronics In Agriculture,* 155, 103-120. https://doi.org/10.1016/j.compag.2018.10.001

TUIK. (2021a). Adrese Dayalı Nüfus Kayıt Sistemi Sonuçları, 2022 (in Turkish). Retrieved April 24, 2023, from https://data.tuik.gov.tr

TUIK. (2021b). Türkiye tarım alanı istatistikleri (in Turkish). Retrieved April 24, 2023, from https://data.tuik.gov.tr

UN. (2013). *United Nations, Department of Economic and Social Affairs, Population Division, Population Estimates and Projections Section*. World population prospects: the 2012 revision. Retrieved April 05, 2023, from http://esa.un.org/unpd/wpp/Excel-Data/population.htm.

WHO. 2011. FAO/WHO guide for application of risk analysis principles and procedures during food safety emergencies. Retrieved April 05, 2023, from https://apps.who.int/iris/handle/10665/44739

Yeniay, E., & Şık, A. (2022). Risk analysis using geographic information systems by determining the factors affecting yield in plant production: a case study from Ankara, Turkey. *Journal Of Agricultural Sciences,* 44-44. https://doi.org/10.15832/ankutbd.900997

Determining temporal and spatial changes in air quality in the city of Nevşehir

Nermin Sari[1] , Fatih Adiguzel*[2]

[1]Nevsehir Haci Bektas Veli University, Institute of Social Sciences, Geography, Nevsehir, Türkiye
[2]Bitlis Eren University Vocational School of Technical Sciences, Transportation Services, Bitlis, Türkiye

Abstract

Air pollution, which has notably surged from the Industrial Revolution onwards, has had adverse effects on all forms of life, primarily humans. Factors such as urbanization, intensified industrial activities, growing production and consumption, and the proliferation of vehicular traffic have significantly contributed to the escalating impact of air pollution. This study aimed to evaluate the levels of particulate matter 2.5, particulate matter 10, and carbon dioxide across diverse locations within Nevşehir city center. Sampling was conducted at ten distinct points, utilizing the CEM DT-9880 device for particulate matter and the EXTECH Easyview 80 CO_2 Analyzer device for carbon dioxide. Measurements were taken during both morning and evening hours to discern daily fluctuations, as well as in both summer and winter to identify seasonal variations. Data collected were input into QGIS software and interpolated to delineate the distribution of pollution throughout the city. The findings reveal that pollution levels are significantly elevated across the city, particularly in industrial zones, organized industrial districts, and densely populated residential regions, as well as in areas where coal is extensively utilized for heating. Conversely, parks and green spaces exhibit the lowest levels of particulate matter and carbon dioxide pollution. While complete eradication of pollutants may be unattainable, it is crucial to mitigate pollutant levels to ensure smooth urban living. To achieve this, installing filters on industrial chimneys, expanding natural gas infrastructure, and promoting the use of natural gas in non-infrastructure areas is essential. Should coal be employed for heating, selecting high-quality, low-soot Siberian coals with high energy content is advisable. Enhancing the city's green areas and parks, as well as expanding afforestation initiatives, holds merit. Efforts to curtail vehicular numbers, encourage public transportation, and prioritize carbon emission-free electric vehicles are crucial for fostering a cleaner urban environment.

1. Introduction

In 1950, approximately 30% of the global population (750 million people) resided in urban areas, a figure that expanded to 47% (2.9 billion people) by 2000. Projections suggest that this urban population will rise to 60% by 2030 and further to 68% by 2050 (United Nations, 2018a; United Nations, 2018b; United Nations, 2018c). European countries exhibit an even higher urbanization rate, with over two-thirds of the total population dwelling in urban regions (Cetin et al., 2019; Cetin et al., 2020; Elsunousi et al., 2021; Cesur et al., 2021; Cetin and Jawed 2021; Cetin & Jawed 2022; Cetin et al., 2022a; Cetin et al., 2022b; Cesur et al., 2022;; Sari et al., 2022; Abo Aisha & Cetin, 2023; Cetin & Abo Aisha, 2023). As per data from the Turkish Statistical Institute (TUIK) in 2022, Turkey's overall population stands at 85,279,553. Of this, 93.4% (approximately 79 million) reside in urban locales, while 6.6% (around 6 million) inhabit rural areas (TUİK, 2022). Notably, migration

represents a pivotal driver behind urban population accumulation in Turkey. Rural-to-urban migration remains an ongoing phenomenon, portending further urban population growth (Kaya, 2010; Cetin et al., 2017a; Cetin et al., 2017b; Kaya et al., 2018a; Kaya et al., 2018b; Cetin et al., 2020; Cetin & Jawed 2021; Cesur et al., 2021; Elsunousi et al., 2021; Cetin & Jawed 2022; Cetin et al., 2022a; Cetin et al., 2022b; Cesur et al., 2022; Sari et al., 2022; Abo Aisha & Cetin, 2023; Cetin & Abo Aisha, 2023).

This perpetual upsurge in urban populations amplifies the significance of ecological equilibrium, clean environments, and comfortable spaces within urban realms. However, the continual surge in urban residents, coupled with escalating population density, concomitant industrialization, and heightened construction and production activities, engenders a multitude of environmental quandaries (Cetin et al., 2019; Cetin et al., 2020; Cesur et al., 2021; Cetin & Jawed 2021; Elsunousi et al., 2021; Cetin & Jawed 2022; Cetin et al., 2022a; Cetin et al., 2022b;; Cesur et al., 2022; Sari et al., 2022; Abo

Cite this article

Sari, N., & Adiguzel, F. (2023). Determining temporal and spatial changes in air quality in the city of Nevşehir. *Advanced GIS*, 3(2), 68-76.

Aisha & Cetin, 2023; Cetin & Abo Aisha, 2023). These environmental challenges entail the degradation of natural ecosystems, air, water, and soil pollution, and the perturbation of ecological harmony (Begum et al., 2008; Kaya, 2010; Brooks & Cetin 2013; Cetin, 2013; Cetin 2015a; Cetin 2015b; Cetin 2016; Kulaç & Yıldız 2016; Deary et al., 2016; Abualqumboz et al., 2017; Cetin et al., 2017a, Cetin et al., 2017b; Sevik et al., 2018; Kaya et al., 2018a; Kaya et al., 2018b; Yucedag et al., 2018).

In urban environments, a spectrum of environmental issues exists, spanning concerns that impact individuals on a personal level to those of mass scale significance. Among these pivotal concerns, air pollution stands out. Air is indispensable for the survival of humans and other living organisms, and its quality must meet certain standards. However, various factors, particularly prevalent in urban settings, lead to a decline in air quality, culminating in the predicament of air pollution (Cetin et al., 2020; Vural, 2021a; Cesur et al., 2021; Elsunousi et al., 2021; Cetin & Jawed 2021; Cetin & Jawed 2022; Cetin et al., 2022a; Cetin et al., 2022b; Cesur et al., 2022; Sari et al., 2022; Abo Aisha & Cetin, 2023; Cetin & Abo Aisha, 2023). At its core, air pollution is a critical environmental challenge arising from the presence of substances (solid, liquid, or gaseous) in the atmosphere that should not be there, or from deviations in the quantities of gases that ought to exist within specific thresholds.

The relentless increase in industrial production, fossil fuel utilization, and vehicular traffic within cities is noteworthy. It is alarming that air pollution levels frequently surpass acceptable thresholds in Turkey, particularly in urban areas (Vural, 2021b). Of the diverse air pollutants, particulate matter emerges as the most recognized and ubiquitous. This pollutant markedly influences human health, as well as the well-being of plants and animals. Carbon Dioxide (CO_2), a greenhouse gas that triggers air pollution and contributes to global warming, has gained significant global attention in recent years. Elevated CO_2 concentrations in urban environments contribute to air pollution. Numerous studies highlight that primary drivers of fluctuating levels in the external environment include traffic density, industrial processes, seasonal shifts, and local weather conditions (Cetin, 2016; Cetin et al., 2017a, Cetin et al., 2017b; Sevik et al., 2018; Türkyılmaz et al., 2018a; Türkyılmaz et al., 2018b; Türkyılmaz et al., 2018c; Türkyılmaz et al., 2018d; Elsunousi et al. Cesur et al., 2021; Cesur et al., 2022a; Cetin et al., 2022b; Cetin et al., 2020; Cesur et al., 2022; Sari et al., 2022; Abo Aisha & Cetin 2023; Cetin & Abo Aisha 2023). Notably, this shift in CO_2 concentrations is predominantly attributable to human activities (Bulgurcu, 2005). Consequently, variations in CO_2 levels manifest in perturbations to people's daily routines and lifestyles. CO_2 concentrations exceeding 1000 ppm result in symptoms such as headaches, fatigue, physical and mental exhaustion, as well as concentration difficulties; surpassing 1500 ppm leads to throat irritation, nasal discomfort, runny nose, coughing, and eye irritation (Ercan, 2012; Cetin et al., 2019; Cetin et al., 2020; Cetin & Jawed 2021; Cesur et al., 2021; Elsunousi et al., 2021 Cetin et al., 2022a; Cetin & Jawed 2022; Cetin et al., 2022b; Cesur et al., 2022; Sari et

al., 2022; Abo Aisha & Cetin, 2023; Cetin & Abo Aisha, 2023). Particulate matter presents considerable hazards to human health, the vitality of plants, and the well-being of animals. These substances can incite cardiovascular ailments, respiratory disorders, and allergic responses (Anderson et al., 2012; Adar, 2014; Mukherjee & Agrawal, 2017; Cetin et al., 2020; Elsunousi et al., 2021; Cetin & Jawed, 2021; Cetin & Jawed, 2022; Cetin et al., 2022a; Cetin et al., 2022b; Cesur et al., 2022; Cesur et al., 2021; Sari et al., 2022; Abo Aisha & Cetin, 2023; Cetin & Abo Aisha, 2023).

This study delved into the dynamics of particulate matter and CO_2 pollutants across diverse zones over the course of a day. The investigation of temporal and spatial variations in these pollutants is of paramount significance in terms of comprehending the damages they inflict and devising strategies for mitigation. The research probed the concentrations of particulate matter and carbon dioxide at ten distinct locations within the urban confines of Nevşehir. Data collection occurred twice daily-once in the morning and again in the evening-and spanned select days during both summer and winter seasons, facilitating an analysis of seasonal shifts. The study sought to unravel the fluctuations in polluting agents within the urban landscape, ultimately presenting solutions grounded in the findings.

2. Materials and methods

This study involved the collection of samples from ten distinct locations within Nevşehir city. Particulate matter measurements in both 2.5 and 10 dimensions, as well as CO_2 measurements, were conducted at specific times of the day across these ten selected points. The data collection took place during mornings (08:30-10:30) and evenings (17:00-19:00). Specifically, measurements occurred over a period of four weeks in February (on Mondays, Wednesdays, and Fridays) during the winter season, and similarly for four weeks in May (on Mondays, Wednesdays, and Fridays) during the summer season.

To facilitate these measurements, 6-channel "CEM DT-9880" devices were employed for particulate matter readings, while "EXTECH Easyview 80 CO_2 Analyzer" devices were utilized for CO_2 measurements. These devices have been employed in numerous other studies as well (Cetin, 2016; Aricak et al., 2016; Cetin et al., 2017a, Cetin et al., 2017b).

Subsequent to the measurements conducted in the study area, the collected data were subjected to analysis through the interpolation method utilizing the open-source QGIS software. This software enabled the development of the most precise models that establish correlations between the measurement points. Within the QGIS software, the Kriging method was employed to process the measurement data

The study area was meticulously chosen to include various settings with diverse characteristics. Ten distinct points were selected within the city, each representing different sources of pollution, including residential, industrial, traffic, and natural origins. The specific points chosen are as follows:
In front of the Provincial Gendarmerie: This location features both a green area and pavement. Its proximity

to the main road led to its selection, with a focus on identifying transportation-related pollution effects.

Parking Area: Notable for its green spaces, this area was chosen to investigate whether plants absorb pollutants.

Housing Area 1: Selected to assess the environmental impact of pollutants originating from residential sources, particularly in densely populated residential zones.

City Center Area: This high-traffic area experiences significant human density throughout the day. It was chosen to determine the impact of human activities on pollution levels.

Industrial Area: Selected for studying the pollution caused by industrial activities.

Green Area: Chosen to explore how green spaces influence pollution intensity.

Housing Area 2: This area contains residences of individuals with slightly lower income levels. Due to this, coal usage for heating is common. It was chosen to analyze how different heating methods affect pollution levels.

Organized Industrial Zone: This location was chosen because of its 24/7 production operations, larger scale compared to other industrial areas, and higher potential for emitting polluting elements.

Intercity Road: Considering the intense pollutants from transportation sources, this road was selected as a representative location.

Housing Area 3: This dense residential area was chosen to assess the pollution levels in another high-density residential setting (Figure 1).

The diverse characteristics of these selected points offer a comprehensive understanding of pollution sources and patterns within the city.
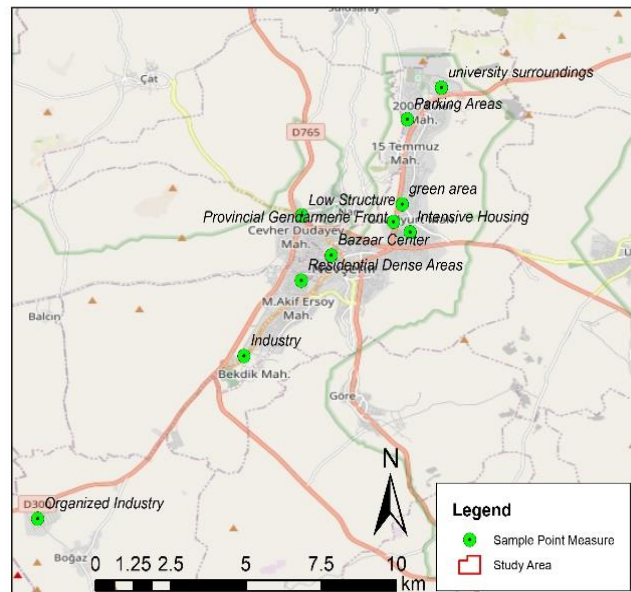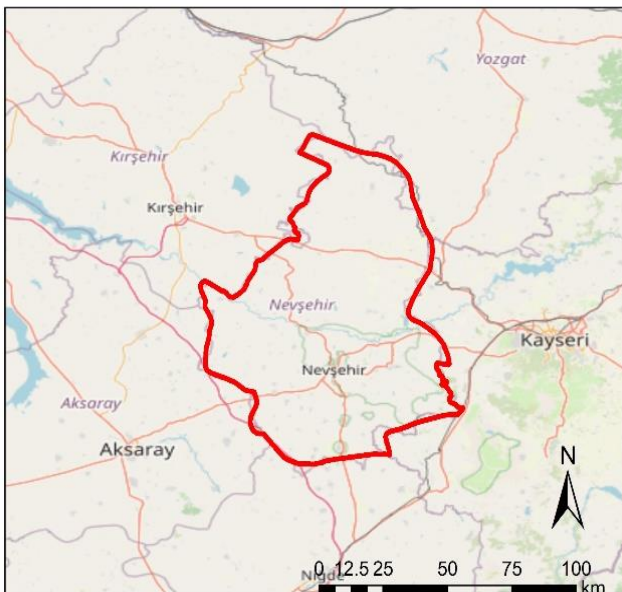

Figure 1. Lokasyon of the study area

3. Results

The averages of measurements conducted during both the morning and evening, as well as across the summer and winter seasons, were computed. The data collected was then subjected to analysis using the QGIS software. These analyses involved interpolation techniques, which in turn were used to generate pollution maps.

Table 1. Averages of the winter season for morning and evening measuring

| Measurement Points	Time	CO_2 ppm	2.5 µm	10 µm
Around of University	Morning	621	103	11
Around of University	Evening	570	190	41
Organized Industrial Zone	Morning	760	236	9
Organized Industrial Zone	Evening	710	369	61
City Center	Morning	570	214	13
City Center	Evening	555	361	64
Housing Areas 1	Morning	450	51	5
Housing Areas 1	Evening	420	59	9
Housing Areas 2	Morning	680	241	16
Housing Areas 2	Evening	640	361	76
Industrial area	Morning	801	541	19
Industrial area	Evening	760	638	9
In front of the Provincial Gendarmerie	Morning	496	123	26
In front of the Provincial Gendarmerie	Evening	445	145	8
Parking Areas	Morning	380	36	10
Parking Areas	Evening	360	49	8
Green Areas	Morning	356	42	28
Green Areas	Evening	320	56	26
Housing Areas 3	Morning	593	109	51
Housing Areas 3	Evening	483	135	81
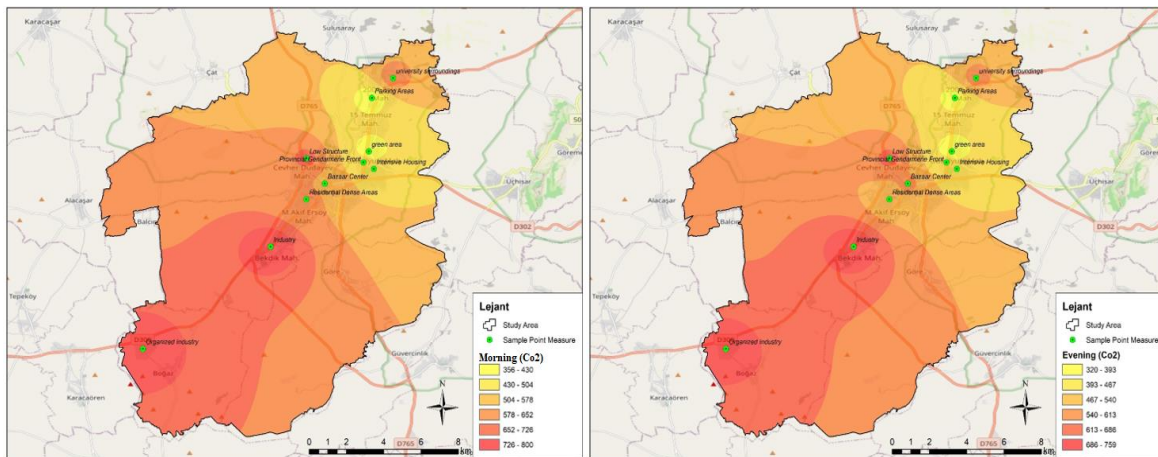
Figure 2. The averages of CO_2 measurement for winter season of morning and evening

In the morning measurement, the highest level of CO_2 was recorded in the industrial zone at a maximum of 801 ppm. This was followed by measurements of 760 ppm in the organized industrial zone and 680 ppm in residential area 2. The lowest CO_2 levels were observed in green areas, with a reading of 356 ppm. Additionally, parking areas displayed relatively low CO_2 levels, registering at 380 ppm. In the evening measurement,

similar trends were observed, with the industrial zone displaying the highest CO_2 levels at 760 ppm. Subsequently, elevated CO_2 levels were recorded in the organized industrial zone and residential area 2, with readings of 710 ppm. In contrast, the lowest CO_2 levels were observed in green areas at 362 ppm during the evening measurement, followed by 360 ppm in park areas (Figure 2).
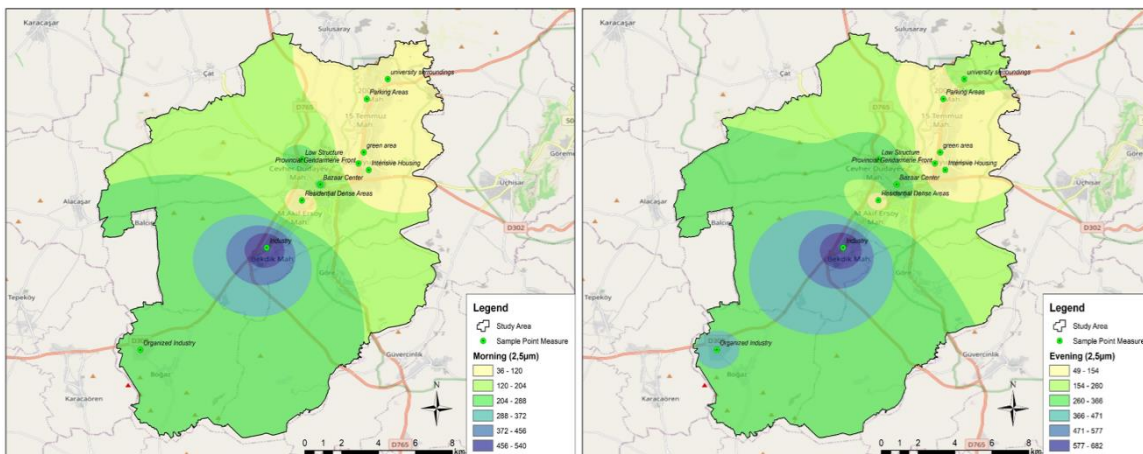

Figure 3. The averages of measurement for winter season of morning and evening 2.5 µm

During the winter measurements, particulate matter with a size of 2.5 μm was measured at the highest levels in the industrial zone, reaching a maximum of 541 μg. Subsequently, elevated levels were observed in residential area 2, recording 241 μg. On the other hand, the lowest concentrations of particulate matter with a size of 2.5 μm were measured in park areas, amounting to 36 μg, followed by 42 μg in green areas.

In the evening measurements, the industrial zone exhibited the highest levels of particulate matter with a size of 2.5 μm, registering 638 μg. Similarly, the organized industrial zone displayed elevated levels, measuring 369 μg. In contrast, the lowest concentrations were observed in park areas (49 μg) and green areas (56 μg) (Figure 3).
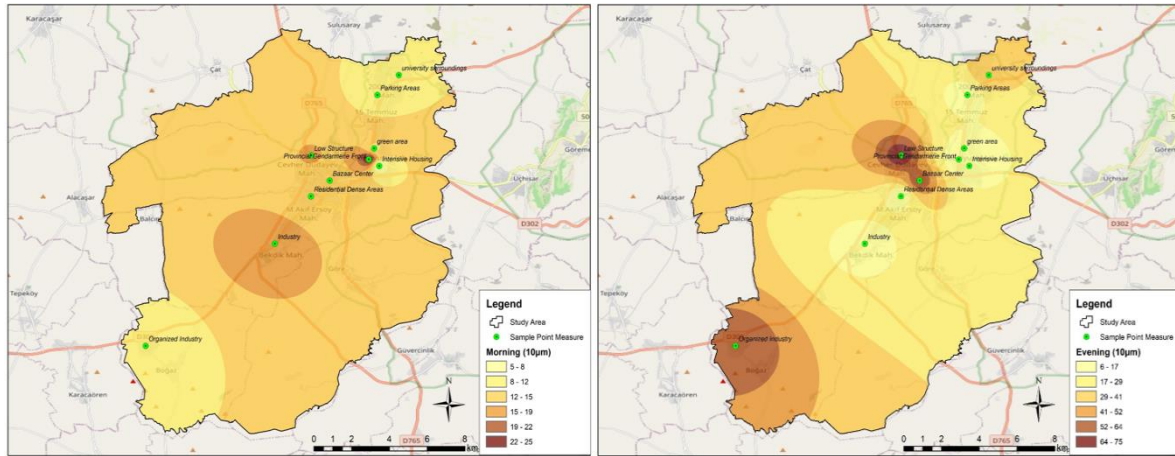

Figure 4. The averages of measurement averages for winter season of morning and evening 10 μm

During the morning measurement in winter, the highest concentration of particulate matter with a size of 10 μm was measured in residential area 3, reaching 51 μg. In contrast, the lowest concentrations were observed in green areas (5 μg) and the organized industrial zone (9 μg).

In the evening measurements, the highest levels of particulate matter with a size of 10 μm were recorded in residential area 3, measuring 81 μg. Conversely, the lowest concentrations were observed in green areas (8 μg) and in front of the provincial gendarme (Figure 4).

Table 2. The averages of measurement averages of the winter season of morning and evening measuring

| Measurement Points	Time	CO_2 ppm	2.5 μm	10 μm
Around of University	Morning	560	95	9
Around of University	Evening	550	160	35
Organized Industrial Zone	Morning	720	210	7
Organized Industrial Zone	Evening	695	330	56
City Center	Morning	550	203	10
City Center	Evening	525	306	56
Housing Areas 1	Morning	430	45	2
Housing Areas 1	Evening	410	55	6
Housing Areas 2	Morning	620	235	12
Housing Areas 2	Evening	630	336	65
Industrial area	Morning	741	461	13
Industrial area	Evening	713	550	8
In front of the Provincial Gendarmerie	Morning	490	106	21
In front of the Provincial Gendarmerie	Evening	440	125	6
Parking Areas	Morning	320	26	9
Parking Areas	Evening	310	45	7
Green Areas	Morning	325	36	9
Green Areas	Evening	315	48	8
Housing Areas 3	Morning	510	96	3
Housing Areas 3	Evening	490	110	6
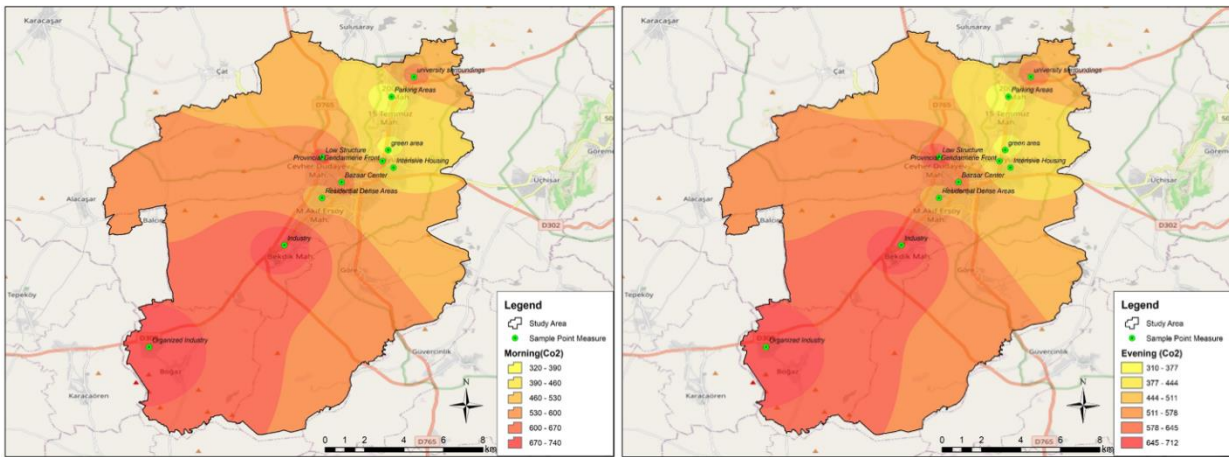
Figure 5. The averages of measurement averages for summer season of morning and evening CO_2

were measured in park areas (320 ppm) and green areas (352 ppm).

During the morning measurement, the highest concentration of CO_2 was recorded in the industrial zone, reaching 741 ppm. Subsequently, elevated levels were observed in the organized industrial zone, measuring 720 ppm. Conversely, the lowest concentrations of CO2

In the evening measurement, similar to the morning measurement, the industrial zone exhibited the highest CO2 concentration, measuring 713 ppm. The lowest CO_2 concentration was measured in parking areas, recording 310 ppm (Figure 5).
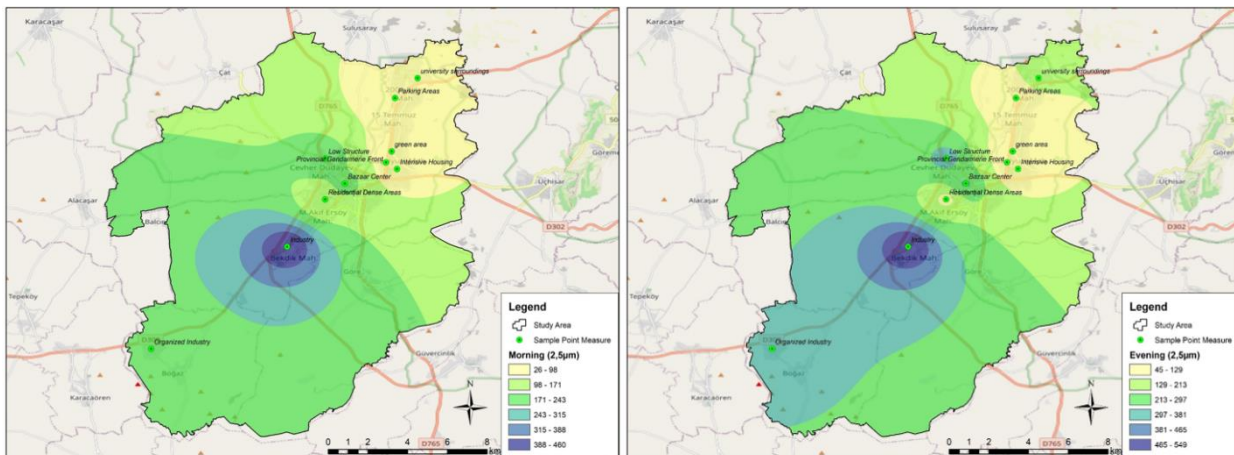

Figure 6. The averages of measurement averages for summer season of morning and evening 2.5 µm

During the morning measurements in the summer season, the industrial zone exhibited the highest concentration of particulate matter with a size of 2.5 µm, reaching 461 µg. Residential areas 2 displayed elevated levels as well, measuring 235 µg. In contrast, the lowest concentration of particulate matter with a size of 2.5 µm was measured in park areas (26 µg) and green areas (36 µg).

In the evening measurements, the industrial zone again recorded the highest concentration of particulate matter with a size of 2.5 µm, measuring 550 µg. Similarly, residential areas 2 exhibited elevated levels, measuring 336 µg. Conversely, the lowest concentrations of particulate matter with a size of 2.5 µm were measured in park areas (45 µg) and green areas (48 µg) (Figure 6).
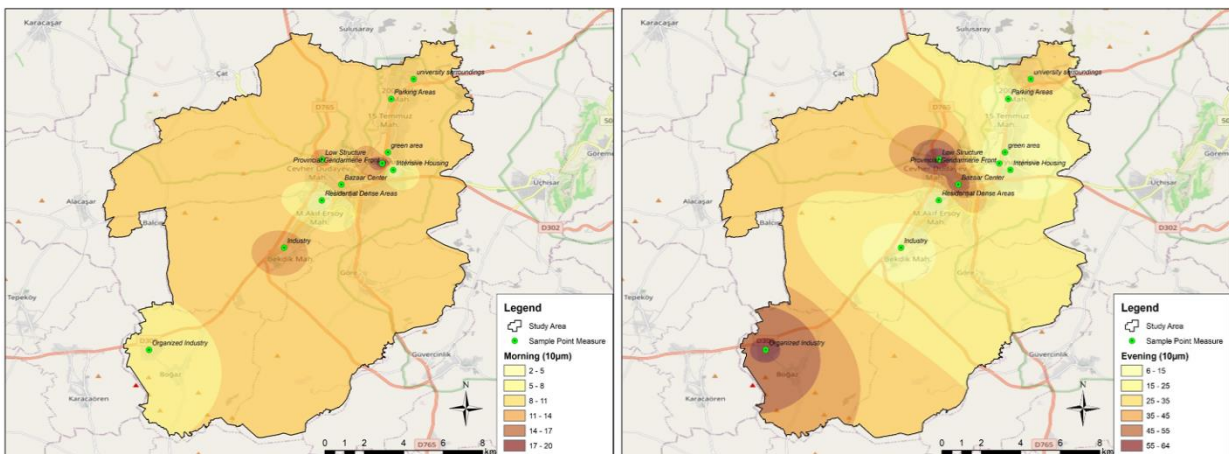

Figure 7. The averages of measurement averages for summer season of morning and evening 10 µm

In the morning measurements during the summer season, particulate matter with a size of 10 μm reached its maximum concentration of 21 μg in front of the provincial gendarmerie. Conversely, the lowest concentrations were measured in residential areas 1 (2 μg) and residential areas 3 (3 μg).

During the evening measurements, the highest concentration of particulate matter with a size of 10 μm was recorded in residential areas 2, measuring 65 μg. On the other hand, the lowest concentrations were measured in residential areas 1, in front of the provincial gendarmerie, and in residential areas 3, all measuring 6 μg (Figure 7).

Throughout the study area, particularly in the industrial zone, organized industrial zone, and residential areas, the levels of CO_2 and particulate matter of sizes 10 and 2.5 μm were observed to be highest. Conversely, the lowest levels were consistently observed in park areas and green areas. The higher concentrations of pollutants in industrial and residential areas can be attributed to the use of fossil fuels for energy and heating. The ability of parks and green areas to absorb pollutants accounts for their reduced pollution levels.

4. Conclusions and recommendations

Air pollution and its impact on air quality have become increasingly significant in recent years. The rise in air pollution levels and the subsequent decline in air quality, primarily driven by human activities, have profound implications for human health as well as the well-being of plants and animals.

Throughout the seasonal and daily measurements conducted within the study area, it was consistently observed that CO_2 levels hovered around 1000 ppm. The recorded maximum values were 796 ppm and 758 ppm, while the minimum values were 385 ppm and 362 ppm. Notably, areas with high human activity exhibited elevated CO_2 levels; Particulate matter concentrations within the study area were particularly high in industrial zones, residential area 2, and the organized industrial zone. Similar to CO_2, human activities are significant contributors to the emission of particulate matter: To mitigate particulate matter and CO_2 levels in urban areas and enhance overall air quality, several measures can be implemented: Install effective filters on factory chimneys within industrial zones and promote the recycling of waste generated from industrial production processes. This will help minimize emissions of pollutants and reduce their impact on the environment for Industrial Filters and Recycling.; Encourage people to use public transportation instead of private vehicles. Reducing the number of vehicles on the road will lead to a relative decrease in pollution generated by traffic and transportation for Promote Public Transportation.; Address pollution caused by solid fuel usage, particularly in areas where low-income individuals reside. Expand the use of natural gas for heating purposes and establish natural gas infrastructure in areas without it. Encouraging the use of higher quality coal for heating can also be beneficial for Improved Heating Practices.

The study indicated that parks and green areas in the city have the ability to absorb air pollutants and act

as buffers. Therefore, the city's green spaces should be expanded and the number of parks increased. Afforestation efforts can further contribute to cleaner air and enhanced urban aesthetics for Expansion of Green Areas.

By implementing these strategies, urban areas can take steps towards achieving better air quality and creating healthier living environments for their residents.

Author Contributions

The contributions of the authors of this article is equal.

Statement of Conflicts of Interest

There is no conflict of interest between the authors.
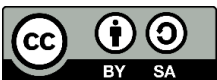
Statement of Research and Publication Ethics

Research and publication ethics were complied with in the study.

References

Abo Aisha, A. E. S., & Cetin, M. (2023). Determination of boron for indoor architecture plants used in indoor architectural designs. *Scientific Research Communications,* 3(2), 15-23. https://doi.org/10.52460/src.2023.007

Abualqumboz, M. S., Mohammed, N. I., Malakahmad, A., & Nazif, A. N. (2017). Investigating indoor concentrations of PM 10 in an underground loading dock in Malaysia. *Air Qual Atmos Health*, 10(2), 147–159. https://doi.org/10.1007/s11869-016-0413-4

Adar, S. D., Filigrana, P. A., Clements, N., & Peel, J. L. (2014). Ambient Coarse particulate matter and human health: A Systematic review and meta analysis. *Current environmental health reports*, 1, 258-274. https://doi.org/10.1007/s40572-014-0022-z

Anderson, J. O., Thundiyil, J. G., & Stolbach, A. (2012). Clearing the air: A review of the effects of matter air pollution on human health *Journal of medical toxicology,* 8, 166-175. https://doi.org/10.1007/s13181-011-0203-1

Aricak, B., Enez, K., Özer Genc, C., & Sevik, H. (2016). A method study to determine buffering effect of the forest cover on particulate matter and noise isolation. *Proceedings Book of 1st International Symposium of Forest Engineering and Technologies (FETEC 2016)*, 177(185).

Begum, B. A., Biswas, S. K., & Hopke, P. K. (2008). Assessment of trends and present ambient concentrations of PM2.2 and PM10 in Dhaka, Bangladesh. *Air Qual Atmos Health,* 1(3), 125–133. https://doi.org/10.1007/s11869-008-0018-7

Brooks, R. M., & Cetin, M. (2013). Water susceptible properties of silt loam soil in subgrades in South West Pennsylvania *International Journal of Modern Engineering Research (IJMER),* 3(2), 944–948.

Bulgurcu, H. (2005). Local heat and energy recovery ventilation equipment design. *Proceedings Book of the 7th National Installation Engineering Congress and Exhibition,* İzmir, Türkiye, 141-150.

Cesur, A., Zeren Cetin, I., Abo Aisha, A. E. S., Alrabiti, O. B. M., Aljama, A. M. O., Jawed, A. A., Cetin, M., Sevik, H., & Ozel, H. B. (2021). The usability of Cupressus arizonica annual rings in monitoring the changes in heavy metal concentration in air. *Environmental Science and Pollution Research,* 28(27), 35642-35648. https://doi.org/10.1007/s11356-021-13166-4

Cesur, A., Zeren Cetin, I., Cetin, M., Sevik, H., & Ozel, H. B. (2022). The use of Cupressus arizonica as a biomonitor of Li, Fe, and Cr pollution in Kastamonu. *Water, Air, & Soil Pollution*, 233(6), 193. https://doi.org/10.1007/s11270-022-05667-w

Cetin, M. (2013). *Advances in Landscape Architecture Environmental Sciences, Chapter 27: Landscape engineering, protecting soil and runoff storm water.* InTech-Open Science-Open Minds, 697–722. https://doi.org/10.5772/55812

Cetin, M. (2015a). Using GIS analysis to assess urban green space in terms of accessibility: case study in Kutahya. *International Journal of Sustainable Development & World Ecology,* 22(5), 420–424. https://doi.org/10.1080/13504509.2015.1061066

Cetin, M. (2015b). *Environment and ecology at the beginning of 21st century, Chapter 55: Using Recycling Materials for Sustainable Landscape Planning.* Kliment Ohridski University Press, 783–788.

Cetin, M. (2016). Sustainability of urban coastal area management: a case study on Cide. Journal of Sustainable Forestry 35(7), 527–541. https://doi.org/10. 1080/10549811.2016.1228072

Cetin, M., & Abo Aisha, A. E. S. (2023). Variation of Al concentrations depending on the growing environment in some indoor plants that used in architectural designs. *Environmental Science and Pollution Research,* 30(7), 18748-18754. https://doi.org/10.1007/s11356-022-23434-6

Cetin, M., & Jawed, A. A. (2021). The chancing of Mg concentrations in some plants grown in pakistan depends on plant species and the growing environment. *Kastamonu University Journal of Engineering and Sciences,* 7(2), 167-174.

Cetin, M., & Jawed, A. A. (2022). Variation of Ba concentrations in some plants grown in Pakistan depending on traffic density. Biomass Conversion and *Biorefinery*, 1-7. https://doi.org/10.1007/s13399-022-02334-2

Cetin, M., Aljama, A. M. O., Alrabiti, O. B. M., Adiguzel, F., Sevik, H., & Zeren Cetin, I. (2022a). Using topsoil analysis to determine and map changes in Ni Co pollution. *Water, Air, & Soil Pollution*, 233(8), 293. https://doi.org/10.1007/s11270-022-05762-y

Cetin, M., Aljama, A. M. O., Alrabiti, O. B. M., Adiguzel, F., Sevik, H., & Zeren Cetin, I. (2022b). Determination and mapping of regional change of Pb and Cr pollution in Ankara city center. *Water, Air, & Soil Pollution,* 233(5), 163. https://doi.org/10.1007/s11270-022-05638-1

Cetin, M., Onac, A. K., Sevik, H., & Sen, B. (2019). Temporal and regional change of some air pollution Parameters in Bursa. *Air Qual Atmos Health*, 12, 311-316. https://doi.org/10.1007/s11869-018-00657-6

Cetin, M., Sevik, H., & Cobanoglu, O. (2020). Ca, Cu, and Li in washed and unwashed specimens of needles, bark, and branches of the blue spruce (Picea pungens) in the city of Ankara. *Environmental Science and Pollution Research,* 27, 21816-21825. https://doi.org/10.1007/s11270-022-05638-1

Cetin, M., Sevik, H., & Isinkaralar, K. (2017a). Changes in the particulate matter and CO_2 concentrations based on the time and weather conditions: the case of Kastamonu. *Oxid Commun* 40(1-II):477–485.

Cetin, M., Sevik, H., & Saat, A. (2017b). Indoor air quality: the samples of Safranbolu Bulak Mencilis Cave. Fresen Environ Bull 26(10), 5965– 5970.

Deary, M. E, Bainbridge, S. J., Kerr, A., McAllister, A., & Shrimpton, T. (2016). Practicalities of mapping PM 10 and PM 2.5 concentrations on citywide scales using a portable particulate monitor. *Air Quality, Atmosphere & Health,* 8, 923–930. https://doi.org/10.1007/s11869-016-0394-3

Elsunousi, A. A. M., Sevik, H., Cetin, M., Ozel, H. B., & Ozel, H. U. (2021). Periodical and regional change of particulate matter and CO_2 concentration in Misurata. *Environmental Monitoring and Assessment,* 193, 1-15. https://doi.org/10.1007/s10661-021-09478-0

Ercan, M. S. (2012). Green glowing environment indicator *X. International Installation Technology Symposium*, İstanbul, Türkiye, 169-175.

Kaya, E., Agca, M., Adiguzel, F., & Cetin, M. (2018). Spatial data analysis with R programming for environment. *Human and ecological risk assessment: An International Journal,* 25(6), 1521-1530. https://doi.org/10.1080/10807039.2018.1470896

Kaya, L. G. (2010). Application of collaborative approaches to the integrative environmental planning of Mediterranean coastal zone: case of Turkey. *Journal of Faculty Bartin Forestry,* 12(18), 21–32.

Kaya, L. G., Kaynakci-Elinc, Z., Yucedag, C., & Cetin, M. (2018b). Environmental outdoor plant preferences: a practical approach for choosing outdoor plants in urban or suburban residential areas in Antalya, Turkey. *Fresenius Environ Bull,* 27(12), 7945–7952.

Kulaç, Ş., & Yıldız, Ö. (2016). Effect of fertilization on the morphological development of European Hophormbeam Ostrya carpinifolia Scop. seedlings. T*urkish Journal of Agriculture: Food Science and Technology* 4(10), 813–821.

Mukherjee, A., & Agrawal, M. (2017). World air particulate matter: Sources, distribution and health effects. *Environmental chemistry letters*, 15, 283-309. https://doi.org/10.1007/s10311-017-0611-9

Sari E, Kaya, L. G., & Çetin, M. (2022). Design Problems and Solution Suggestions in Bridge Intersections: The Case Study of Democracy Bridge Intersection, Antalya-Turkey (Köprülü Kavşaklarda Tasarım Sorunları ve Çözüm Önerileri: Antalya Demokrasi Köprülü Kavşağı Örneği – in Turkish *The Journal of Graduate School of Natural and Applied Sciences of Mehmet Akif Ersoy University,* 13(1), 81-92. https://doi.org/10.29048/makufebed.1067284

Sevik, H., Ozel, H. B., Cetin, M., Ozel, H. U., & Erdem, T. (2018). Determination of changes in heavy metal accumulation depending on plant species, plant organism, and traffic density in some landscape plants. *Air Quality, Atmosphere & Health,* 12, 189-195. https://doi.org/10.1007/s11869-018-0641-x

TUİK. (2023). *Turkish Statistical Institute (TUİK).* Retrieved August 10, 2023, from https://biruni.tuik.gov.tr/medas/?kn=130&locale=tr

Türkyılmaz, A., Cetin, M., Şevik, H., Işınkaralar K., & Ahmaida Saleh, E. A. (2018a). Variation of heavy metal accumulation in certain landscaping plants due to traffic density. *Environment, Development and Sustainability,* 22, 2385-2398. https://doi.org/10.1007/s10668-018-0296-7

Türkyılmaz, A., Şevik, H., & Cetin, M. (2018b). The use of perennial needles as biomonitors for recently accumulated heavy metals. *Landscape and Ecological Engineering,* 14(1), 115–120. https://doi.org/10.1007/s11355-017-0335-9

Türkyılmaz, A., Şevik, H., Cetin, M., & Ahmaida Saleh, E. A. (2018c). Changes in heavy metal accumulation depending on traffic density in some landscape plants. *Polish Journal of Environmental Studies*, 27(5), 2277–2284. https://doi.org/10.15244/pjoes/78620

Türkyılmaz, A., Şevik, H., Isinkaralar, K., & Cetin, M. (2018d). Using Acer platanoides annual rings to monitor the amount of heavy metals accumulated in air. *Environmental monitoring and assessment*, 190(578), 1-11. https://doi.org/10.1007/s10661-018-6956-0

United Nations. (2018a). *World Urbanization Prospects.* Retrieved June 29, 2023, from https://population.un.org/wup/Publications/Files/WUP2018-Report.pdf

United Nations. (2018b). *World Urbanization Prospects.* Retrieved June 29, 2023, from https://population.un.org/wup/Publications/Files/WUP2018-Highlights.pdf

United Nations. (2018c). *World Urbanization Prospects.* Retrieved June 29, 2023, from https://population.un.org/wup/Download/

Vural, E. (2021a). Air quality change related to related to particulate matter in some selected green areas in Sanliurfa. *Kastamonu University Journal of Engineering and Sciences,* 7(1), 19-26.

Vural, E. (2021b). Güneydoğu Anadolu Bölgesi İllerinin CBS Kullanarak Hava Kalitesinin Mekansal Değişiminin İncelenmesi. *Journal of Natural Hazards and Environment,* 7(1), 124-135. https://doi.org/10.21324/dacd.718450

Yucedag, C., Kaya, L. G., & Cetin, M. (2018). Identifying and assessing environmental awareness of hotel and restaurant employees' attitudes in the Amasra District of Bartin. Environmental Monitoring and Assessment, 190, 60. https://doi.org/10.1007/s10661-017-6456-7